UNIVERSITÄT
BERN

OESCHGER CENTRE
CLIMATE CHANGE RESEARCH

Temperature-mortality projections under climate change scenarios in Peru

Master's Thesis

Master program in Climate Sciences
Climate Change and Health Group, Institute of Social and Preventive Medicine
Faculty of Science, Universität Bern

handed in by

Katia Karen Hidalgo Olvera
21-116-074

Principal supervisor

Prof. Dr. Ana María Vicedo-Cabrera

Co-supervisor

Dr. Santos José González Rojí

Advisors

Dr. Evan De Schrijver and Dr. Coral Salvador

2024

Preface

Exposure to non-optimal ambient temperatures has been categorized as a global burden and risk to human health [1]. In 2021, non-optimal temperatures were reported to cause more than 5 million deaths per year [2]. Projections indicate that this estimate will rise as heatwaves and higher temperatures are expected to become more common [3]. Thus, quantification of the current and future impacts of extreme heat and cold is important to identify vulnerable areas and exposed populations. While extensive research has quantified temperature-related mortality in countries of the Global North, studies focusing on the Global South, have been limited, sometimes, due to the absence of data. Africa, Southeast Asia and Latin America are the regions where the least research has been conducted. Nonetheless, in Latin American countries, temperatures have already increased by approximately 0.2°C per decade [4]. By mid-century, the Latin America and Caribbean region is expected to reach a population of 736.9 million inhabitants [5]. Thus, assessing the association between temperature and mortality in the region is key. By quantifying both current and projected temperature-related mortality, it is possible to identify areas where the risk is higher, which is essential for developing effective public health strategies to reduce the vulnerability of exposed populations.

To our knowledge, in Latin America, there are no nationwide analyses quantifying temperature-related mortality fractions at a state level. To address this research gap, in this Master's thesis we analysed 1,156,601 deaths that occurred between 2009 and 2019 across Peru. Here, we obtained the temperature-mortality association at a department level, including all Peruvian provinces. Then, we computed the relative mortality risk associated to non-optimal temperatures at a national level, as well as for various subgroups, including sex, age and the six main causes of death using a multilevel multivariate meta-regression model. Furthermore, we derived the temperature-mortality associations as the Best Linear Unbiased Predictions (BLUPs) at a department level. We used BLUPs to derive the location-specific

Minimum Mortality Temperature (MMT), which we then used to calculate the mortality fraction attributed to non-optimal ambient temperatures in each Peruvian department.

Moreover, we also projected the temperature-mortality association for three Peruvian departments using log-linear extrapolation. This allowed us to estimate temperature-related mortality in the future under a mitigation (Representative Concentration Pathway-RCP 2.6) and a high emissions scenario (RCP 8.5). Our results indicated that out of the 1,156,601 recorded deaths between 2009 and 2019, 8.77% were linked to non-optimal temperatures. We found that the majority of excess mortality was cold-related. However, for future conditions, under both mitigation (RCP 2.6) and high emissions (RCP 8.5) scenarios, we found that heat-related mortality is projected to surpass cold-related mortality.

This master's thesis project consisted of two main parts. The first one focused on quantifying the effects of non-optimal ambient temperatures at a department level from 2009 to 2019. The findings of this analysis are presented in Chapter 2 of this document, in the form of a research article, which will be submitted to the Environmental Epidemiology journal. The second part of the project focuses on the projected temperature-related mortality for the years 2071 to 2099 across three Peruvian departments. These results are illustrated and described in Chapter 3. The remaining chapters of this document are as follows: Chapter 1 explains the context, goals, data, and methodology of this thesis. Chapter 4 presents the conclusions and key findings of the analysis. Chapter 5 contains the references for all sources cited in this document.

Contents

List of Figures

Introduction

Manuscript

List of Tables

Manuscript

Projected health impacts in the long-term future

Appendix A

Abbreviations

CI	Confidence Interval
°C	Degree Celsius
DLNM	Distributed lag Non-Linear Model
ICD	International Classification of Diseases
INEI	National Institute of Statistics and Informatics of Peru
MINSA	Ministry of Health of Peru
MMT	Minimum Mortality Temperature
MMP	Minimum Mortality Temperature Percentile
PISCOt	Peruvian Interpolated data of the SENAMHI's Climatological and Hydrological Observations
QM	Quantile Mapping
RCP	Representative Concentration Pathway
RR	Relative Risk
WRF	Weather Research and Forecasting Model

Chapter 1

Introduction

1.1 Overview

Robust and thriving environments influence the well-being and health outcomes of the populations that inhabit them. However, human activities have driven changes in the climate and environmental dynamics, negatively impacting ecosystems' functions and leading to the emergence of new hazards for human health [3]. In 2019, it was estimated that climate-sensitive diseases accounted for 69.9% of the total annual deaths [6, 7], and, by 2050, the projections indicate that 250,000 additional deaths per year will be attributable to climate-related hazards [6].

The Intergovernmental Panel on Climate Change (IPCC) [3] has reported that the frequency and severity of heatwaves and higher temperatures have increased since the 1950s, while the occurrence of lower temperatures and cold waves has decreased. Even though this trend suggests that exposure to cold extremes will be less prevalent in the future, at present, most of the global temperature-related mortality is linked to non-optimal cold temperatures [2]. This has been confirmed by numerous authors and research groups who have quantified the excess of heat and cold-related mortality in different regions of the world. [8–15].

Heat-related mortality has contributed the least to temperature-related mortality through the years. Nevertheless, during the boreal summer, 37% of global heat-related deaths can be attributed to anthropogenic climate change [16]. Moreover, it is projected that in the future heat-related deaths will surpass and outweigh the mortality burden related to colder temperatures [17–22]. Although temperature-

related mortality occurs due to several factors and can be highly influenced by socioeconomic factors, elderly and young individuals are the most affected. Especially among elderly individuals, exposure to extreme heat and cold can enhance underlying health conditions, increasing their risk of mortality [6]. Nonetheless, consistent exposure to non-optimal temperatures can disrupt the body's ability to maintain thermal homeostasis in individuals across all age groups and populations, potentially leading to hypothermia or hyperthermia [23, 24].

1.2 Regulation of the body temperature

In theory, individuals exposed to dry ambient temperatures ranging from 12.7 °C to 54.4 °C can maintain an optimal core body temperature [25]. However, tolerance to high and low temperatures varies depending on the frequency, duration of exposure, ambient conditions and activities performed. As homeotherms, humans can control and keep the internal core body temperature through physiological thermoregulation [23], independently of ambient conditions [26–28]. Nonetheless, air temperature directly influences the temperature of the skin potentially impacting the core body temperature regulation. The core body section is formed by the most vulnerable and vital organs located in the head, thorax and abdomen [26, 27], while the skin, subcutaneous tissues and limbs shape the outer body shell [27, 29]. Although the core body section is crucial for maintaining homeostasis, the body shell exchanges information with the environment, which later is sent to the hypothalamus [26].

The hypothalamus controls the main temperature receptors [27], ensuring the stability of the core body temperature by balancing heat loss and heat production [26, 30]. In healthy individuals, the physiological thermoregulation keeps the core body temperature at 37 °C with a range of ±0.6 °C [25, 30, 31]. When the physiological regulation fails, the body can experience core body temperatures below 35 °C resulting in hypothermia [32], or hyperthermia, if the core body temperature rises above 38 °C [33]. In more severe cases, when the core body temperature increases from 40.5 °C to 42.2 °C, heat stroke occurs [25]. However, in individuals who carry out hard labour, the tolerance to heat is reduced, increasing the risk of heatstroke if temperatures exceed the range of 29.4 °C to 32.2 °C [25]. Moreover, ambient factors like humidity also influence the risk of heatstroke. When air temperatures rise above 34.4 °C and there is a 100% of humidity, or the skin is wet, the core body temperature increases faster [25]. This occurs due to hidromeiosis, a reduced ability of eccrine glands to secrete sweat in humid conditions [34–36].

When the human body is exposed to extreme heat, heat dissipation occurs through radiation, convection, evaporation, and conduction [30, 37]. If the skin temperature surpasses the ambient temperature, the body temperature is balanced by losing heat through evaporation (sweating). In most cases, sweating occurs when the air temperatures are higher than 36 °C [26], however, other studies have reported that individuals start sweating when air temperatures are above 30 °C [38]. In addition to sweating, the body releases heat by increasing blood flow to the skin and active muscles [39]. However, the blood flow diversion can elevate the heart rate and reduce the blood circulation for vital organs, raising the risk for individuals with preexisting cardiovascular diseases [24, 39].

In comparison, when the air temperature is lower than the skin temperature, the body responds by increasing heat production and minimizing heat loss through radiation and conduction [25, 26]. When the hypothalamus receives signals of extreme cold, it triggers the vasoconstriction and shivering responses [40]. Additionally, if necessary, the body increases heat production throughout non-shivering thermogenesis and higher catecholamine secretion [30, 37]. Nevertheless, the balance between heat production and heat loss varies among individuals because the metabolism changes as we age. Elderly individuals and young infants have a lower capacity to maintain and generate heat in cold temperatures [26]. Children and infants, whose metabolism is still developing, are more susceptible to extreme heat [24, 41, 42]. Meanwhile, older adults have a lower tolerance to heat [43] due to fewer eccrine glands, which limit their sweat production [28].

The tolerance to heat and cold can change over time. Constant exposure to heat or cold ambient temperatures leads to acclimatization, which is crucial in how the body can adapt to both heat and cold environments [25, 26, 44]. Acclimatization to warm environments enhances the ability of the body to dissipate heat by increasing sweat production, which can start at a lower core body temperature than usual [26]. Conversely, cold acclimatization reduces the transfer of heat from the core parts of the body to the skin [26]. However, acclimatization alone is not enough to cope with extreme and non-optimal ambient temperatures. In addition to all the physiological mechanisms that our body has to regulate the body temperature, behavioural thermoregulation allows humans to live and adapt to different climates. By modifying our living environment, we can effectively control our body temperature. The type of clothing we wear also allows us to regulate heat production and loss, maintaining comfort. The sensory information that our skin registers is crucial, as any

signal of discomfort due to overheating or chillness is sent to the hypothalamus [26, 27]. This initiates responses that not only lead to physiological thermoregulation but also drive behavioural adjustments. Nevertheless, access to amenities like air conditioning, proper housing insulation, affordable accommodation, and adequate clothing is limited for some populations. This lack of resources can lead to inadequate responses to non-optimal temperatures, increasing the vulnerability of exposed populations and raising the risk of temperature-related mortality.

1.3 Vulnerability of Latin America and Peru

By the end of 2023, Latin America had an approximate population of 652.3 million [5]. Within the total population, approximately 33 million people faced poverty [45], having limited access to housing, sanitation, drinking water and other basic services. The Latin American region is the second-highest disaster-risk area in the world [46], many countries of the region are highly prone to natural disasters because of their geographical location. However, highly populated urban areas, limited economic growth, violence, political instability, mass migration, inequality and poverty exacerbate the vulnerability of the region [46].

Between 2000 and 2022, natural hazards affected 190 million Latin Americans, including 5.6 million who were negatively impacted by extreme temperatures [46]. In addition, Latin American countries are responsible for less than 5% of the CO_2 emissions [47]. Nevertheless, according to the World Meteorological Organization [4], temperatures in Latin America and the Caribbean have increased at an average rate of approximately 0.2 °C per decade from 1991 to 2021. Without adaptation measures in the region, climate change is projected to cause 5,613 heat-related deaths by 2030, a number that is expected to rise to 18,135 by 2050, affecting mainly individuals over 65 years old [48].

In 2023, Peru had a total population of more than 33 million inhabitants [49]. Around one-third of the Peruvian population lives in areas exposed to frequent environmental hazards [50]. Based on the available data, in 2021, approximately 10 million individuals were categorized as vulnerable and at risk of experiencing poverty, mainly in the urban areas [51, 52]. Although there are no recent estimates, in 2014 more than 7 million Peruvians were exposed to non-optimal cold temperatures [50, 53]. Between 2008 and 2015, 6.8% of temperature-related deaths in Peru were cold-related [13, Supplementary Material], while only 0.9% were reported to be heat-

related. In 2020, it was reported that 360,000 children in Peru were exposed to high heatwave frequency, a number projected to increase to 5.4 million by 2050 under an Shared Socioeconomic Pathway - SSP1 scenario [54]. Around 10 million Peruvians are projected to experience extreme heat if global temperatures rise by 2 °C or more [50, 55]. Under the SSP5-8.5 climate-population scenario, a global temperature increase of 2°C is projected to result in a 1.2% [95% CI: 3.5% to 4.9%] increase in heat-related mortality in Peru [56, Supplementary Material]. If temperatures rise by 3°C, heat-related mortality is expected to rise by 2.2% [95% CI: -14.7% to 16.2%] [56, Supplementary Material].

1.4 Motivation and study aim

Projections indicate that Peru will be more exposed and experience heatwaves more frequently by the end of the century [50]. Nonetheless, only a few studies have quantified the future impacts of non-optimal temperatures in the country. Studies conducted by Chen et al. [56] and Vicedo et al. [16] have quantified the potential temperature-mortality burden under future conditions in Latin America using data from the Multi-Country MultiCity (MCC) Collaborative Research Network. Zhao et al. [2] also used the MCC database to quantify cold- and heat-related mortality, focusing on the period from 2000 to 2019. Additionally, Kephart et al. [13], and Bakhtsiyarava et al. [57] have also studied the effect of extreme temperatures on mortality in Latin America, focusing on city-level impacts using data from the Salud Urbana en América Latina (SALURBAL) project. These authors and research groups have conducted significant and valuable research quantifying temperature-related mortality in Latin America, with each study including an analysis of some Peruvian locations. However, to the best of our knowledge, none of the research has estimated temperature-related mortality at a department level including all Peruvian provinces.

To address this research gap, here we examined the location-specific temperature-mortality associations at a departmental level and quantified cold and heat-related mortality fractions for the years 2009 to 2019. Additionally, we estimated the projected excess temperature-related mortality under a high and low emissions scenario for the departments of Ica, Madre de Dios and Ucayali for the period 2071 to 2099.

Our study framework was guided by the following research questions and study goals:

1.4.1 Research questions

- Are non-optimal temperatures an environmental stressor that influences mortality in Peru?
- Will heat- and cold-related mortality increase or decrease in Peru in the future under a low and high emissions scenario (RCP 2.6 and 8.5)?

1.4.2 Study goals

- Examine the relationship between temperature and mortality to identify the potential impact of non-optimal ambient temperatures.
- Quantify the health burdens associated with non-optimal temperatures for all Peruvian departments.
- Assess and quantify future health burdens associated with projected non-optimal temperatures.

1.5 Research approach

This master's thesis was structured into two main parts, and it followed the methodology described by Vicedo et al. [58] and the small-area approach of Gasparrini [59]. Figure 1 illustrates all the processes and analyses conducted in this study. To ensure uniform color representation, all figures were generated in R using the `scico` package [60].

- The first part of the project focused on obtaining the association between daily mean temperatures and daily mortality for each department of Peru. These associations were obtained by analysing all-cause mortality across the entire Peruvian population. Also, the exposure-response estimates were calculated for different subgroups. The subgroups were formed by grouping mortality counts based on the same age group, sex, and cause of death. The age groups were divided into individuals under 65 years old and those aged 65 and older. This is further explained in the methodology section. The temperature-mortality associations were used to obtain the Minimum Mortality Temperature (MMT) and to quantify the attributable mortality fraction due to non-optimal heat and cold. The results are presented in Chapter 2 in the form of a research article, which will be submitted to the journal Environmental Epidemiology.

The first part of the thesis involved the following tasks:

1. Conceptualization of the project.
2. Request of mortality data to the Ministry of Health of Peru [Ministerio de Salud del Peru] (MINSA).
3. Aggregation of mortality data for all 196 Peruvian provinces from 2009 to 2019.
4. Linkage of daily mortality counts with daily mean temperature that was obtained from the PISCOt v1.2 dataset provided by Huerta et al. [61].
5. Implementation of the first-stage analysis using the small-area analysis approach described by Gasparrini [59].
6. Quantification of the attributable mortality fraction due to heat or cold for all departments of Peru.

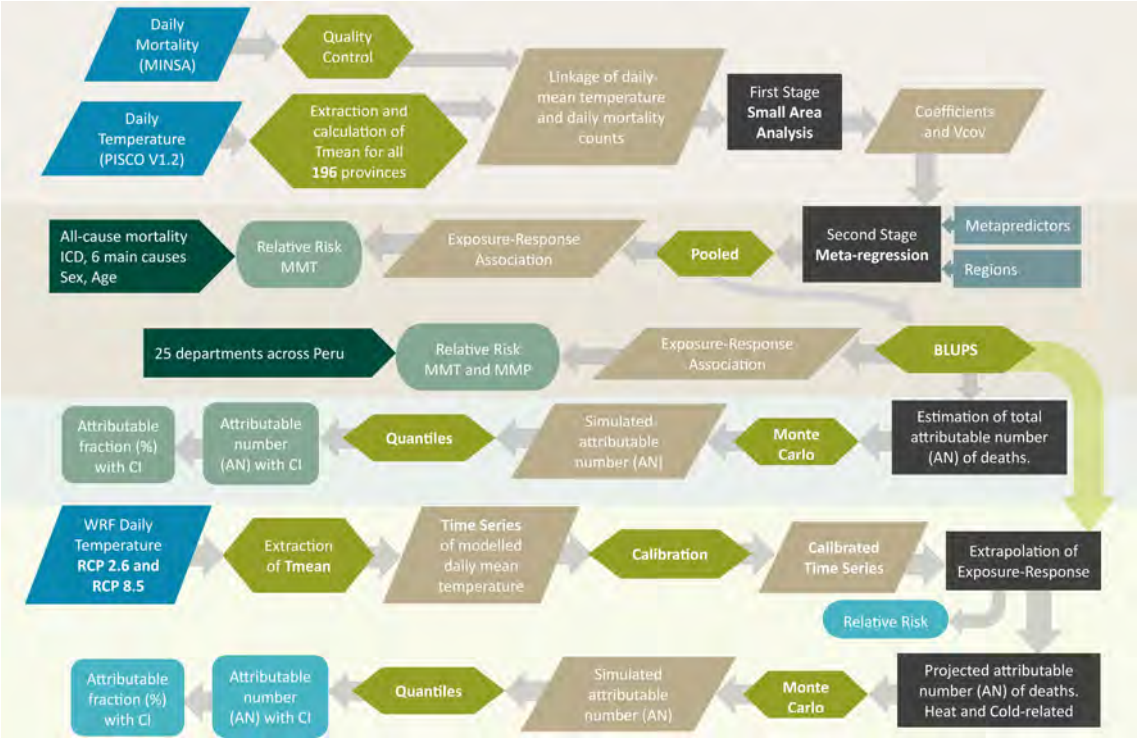

Figure 1: Modelling framework flowchart. The flowchart illustrates the process that was followed for the master's thesis. The parallelograms indicate the inputs and output data. The hexagons show the processes. The black rectangles indicate the main statistical analyses that were performed. The main outcomes are illustrated with rounded rectangle shapes. The four different shades in the background of the figure show the different phases of the study.

- The second part of this thesis aimed to estimate the future attributable mortality fraction due to projected changes in temperature under a mitigation (RCP 2.6) and high emission (RCP 8.5) scenario for the period 2071 to 2099. The results are described and illustrated in Chapter 3. The outcomes of the second-stage analysis obtained in the first part of this thesis were used to log-linearly extrapolate the temperature-mortality associations. The extrapolation was done for three departments, Ica, Ucayali and Madre de Dios, and the results were used to quantify the future cold- and heat-related mortality.

  The tasks for this part of the thesis were the following:

  1. Curation of three climate datasets that included daily mean temperature simulations for the historical (1981-2010) and future period (2071-2099) under RCP 2.6 and RCP 8.5 climate scenarios.

  2. Extraction of temperature values and generation of two daily-mean temperature time series.

  3. Bias-correction of the temperature time series with the approach described by Hempel et al. [62] and used in the methodology published by Vicedo et al. [58].

  4. Log-linear extrapolation of temperature-mortality associations.

  5. Estimation of projected attributable mortality fractions due to non-optimal temperatures.

1.5.1 Research setting

For the observed period, from 2009 to 2019, temperature-related mortality was obtained for all Peruvian departments. However, due to the limited spatial coverage of the future regional climate simulations at high resolution, the projections for the period 2071 to 2099 were calculated only for the departments of Ica, Madre de Dios and Ucayali. Peru is divided into three administrative levels: departments [departamentos], provinces [provincias] and districts [distritos]. The smallest administrative units in Peru are the districts, which are grouped into provinces, the second-level administrative divisions. The departments are the biggest administrative division in the country. In 2020, the National Institute of Statistics and Informatics of Peru [63] reported that the country had 1,874 districts, 196 provinces and 25 departments, which, to our knowledge, has not changed. Although districts are the smallest ad-

ministrative divisions, for this thesis, we used provinces as the smallest unit for our analysis.

For the first part of the analysis, we used the time series small-area approach described by Gasparrini [59]. Therefore, daily mortality counts reported at the district level were aggregated by province. A detailed explanation is described in the methodology section. Figure 2a shows the division of all 25 Peruvian departments, where each department is highlighted with a different colour. The provinces within each department are indicated by grey lines. Figure 2b on the right highlights the departments of Ica, Madre de Dios and Ucayali, which we analysed for the future period from 2071 to 2099.

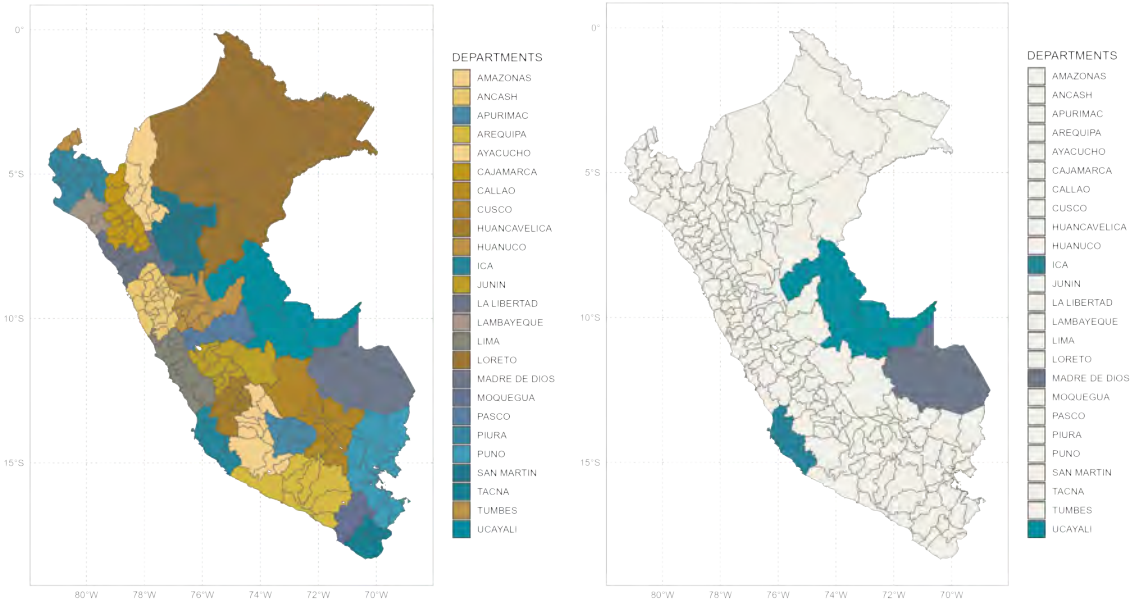

(a) Study area for the period 2009-2019 **(b)** Study area for the period 2071-2099

Figure 2: Study areas for the observed and future periods

1.5.2 Data

For this project, we used three main datasets. Two of them were climate datasets and one was a curated mortality dataset. For the analysis of the observed period (2009-2019), we used the PISCOt v1.2 dataset by Huerta et al. [61] and the mortality counts provided by MINSA. To quantify the future excess mortality for the period from 2071 to 2099, we used temperature simulations generated by González-Rojí et al. [64].

High-resolution daily-scaled air temperature dataset, PISCOt v1.2

The high-resolution daily temperature dataset by Huerta et al. [61] includes NetCDF files with average, maximum, and minimum daily temperatures at various spatial resolutions from 1991 to 2020. The files are available in the following repository: `https://doi.org/10.6084/m9.figshare.c.5959863.v3`. For this project, we used files containing daily values of maximum and minimum temperatures at a 0.05° spatial resolution (approximately 5 km) for the years 2009 to 2019. We extracted and calculated the daily mean temperature for each province and department using official geospatial data from the National Geographic Institute of Peru. The shapefiles are accessible at the following link: `https://www.idep.gob.pe/geovisor/descarga/visor.html`. We used the most recent version available as of April 5, 2023. The extraction and calculation of the daily mean temperature were performed using the `exact_extract` function from the *exactextractr* [65] package in R.

Daily mortality counts, data collected by MINSA

The Ministry of Health of Peru provided the daily mortality counts for all of Peru from 2009 to 2019. The information was delivered in electronic form and contained the following:

- Date of death
- Sex
- Age
- Administrative division where the death occurred
- ICD code referring to the cause of death

Before the analysis, the data was curated and a quality control was performed to ensure completeness and consistency of the information. The curated dataset consisted of 1,155,753 recorded deaths. Due to the aim of our analysis, we aggregated the mortality counts into 196 provinces and grouped the information into 25 lists.

Daily mean temperature data, simulations for the period of 2071-2099

For the second part of the master's thesis, the future temperature-mortality estimates were obtained using bias-corrected daily mean temperature simulations. The future daily temperature values were generated employing the Weather Research and Forecasting Model (WRF) [66], a dynamical downscaling model. Outputs from

the Community Earth System Model (CESM) were used as inputs for WRF to simulate both a mitigation and a high-emission scenarios (RCP 2.6 and 8.5, respectively). The horizontal domains for the simulations incorporated spatial resolutions of 25 km, 5 km and 1 km. To reduce the biases of the climate simulations, the outputs were bias-corrected using the quantile mapping (QM) approach, which we used for this project. This information was provided in three files as NetCDF. One file contained historical temperature values from 1981 to 2010, another included data from 2071 to 2099 under RCP 2.6, and the last dataset contained data from 2071 to 2099 under RCP 8.5. Figure 3 shows the areas covered by the 5 km and 1 km domains. Due to the focus of our study, we used the data with 5 km resolution, which fully covered most of the southern Peruvian departments and, allowed us to analyse the areas of Ica, Madre de Dios and Ucayali.

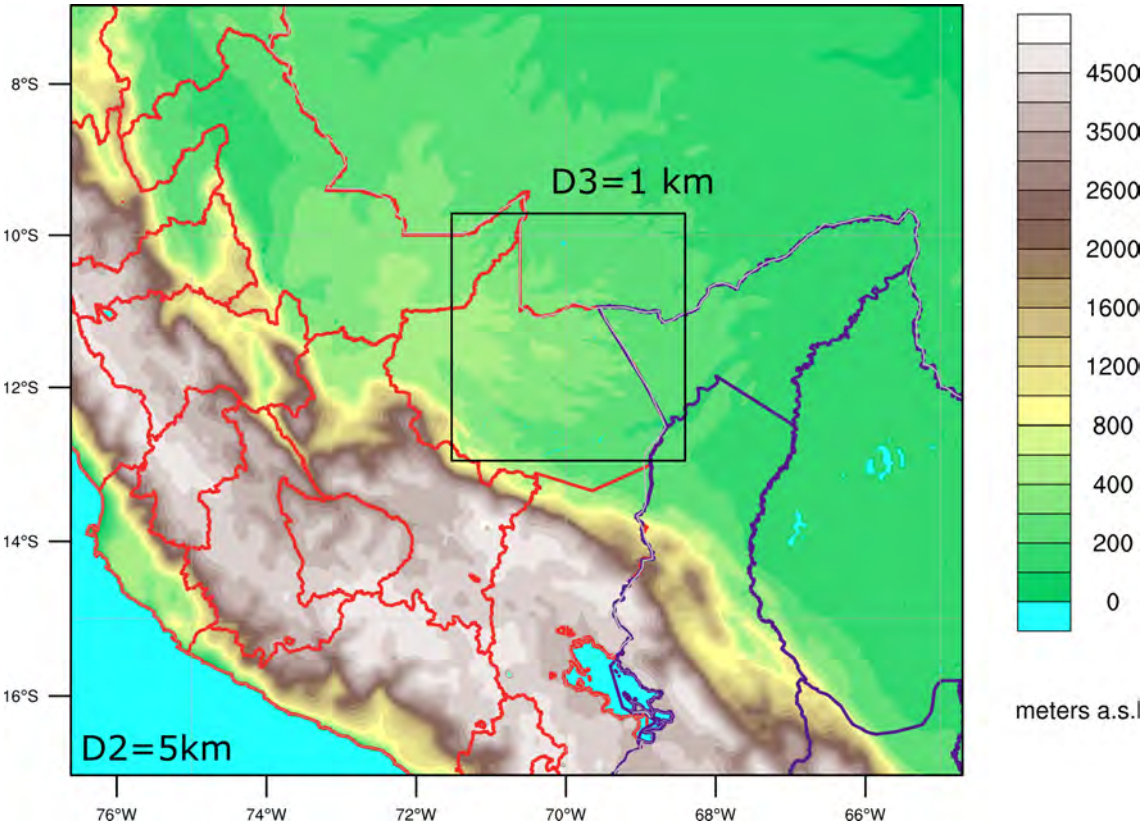

Figure 3: Domains at 5 km and 1 km that were used for the climate simulations with WRF. The departments of Peru are marked in red, and the ones for Bolivia in blue. González-Rojí et al. [64]

Before extracting the temperature values to generate the daily time series of projected temperatures, we curated the datasets of the simulated daily mean temperature. First, we adjusted the projected geographical coordinates of the climate

datasets using Python. Later, we extracted the temperature values for each department using the `exact_extract` function in R from the *exactextractr* package [65]. Afterwards, the daily mean temperatures were used to generate two time series. Each series included historical values for the period 1981 to 2010, as well as the future temperatures from 2071 to 2099, under either RCP 2.6 or RCP 8.5 conditions.

Data linkage, case time series for small-area analysis

The linkage procedure for the observed period was done following the methodology of Gasparrini [59]. The extraction of the mortality and observed climate data was done following the geographical boundaries of each province. As described before, the daily mean temperatures and daily mortality counts were organized as time series. Each series had common column names and values indicating the province and department names that allowed us to link both, daily mortality and mean temperature. The linkage was done using the `merge( )` function from the *base* package [67] in R. Figure 4 shows an example of the temperature and mortality time series for the observed period (2009-2019).

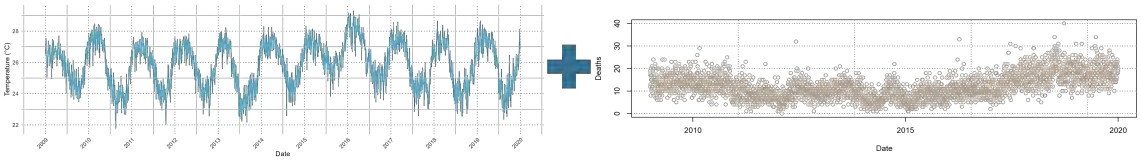

Figure 4: Data linkage between the daily mean temperature (left) and daily mortality (right).

Data preparation, quantification of the future impacts

For the analysis of the future impacts, we first calibrated the future temperature time series using the function `fhempel( )` in R. The function conducts a correction of the series by re-aligning the simulated temperature values with observed data. The function is based on the methodology of Hempel et al. [62]. The calibration procedure keeps the variability of the simulated temperature and corrects biases due to deviations in the modelling procedure. To calibrate the series with projected temperatures, we used temperature values obtained from the PISCOt v1.2 dataset. We used five years to calibrate the series, from 2005 to 2010, and conducted a sensitivity analysis using information from five years prior as well. After, we generated future baseline mortality series for each of the departments that we analysed. To generate the baseline mortality series, we computed the average of deaths for each day of the year, using the observed daily mortality data.

1.5.3 Statistical analysis

Because we had access to daily mortality counts at a district level and high-resolution daily mean temperature values, we were able to conduct an extended two-stage case time series analysis for small geographical areas. The approach is described in detail by Gasparrini [59]. We used this methodology to study the observed period from 2009 to 2019. However, to quantify the future mortality burden, we followed the "Modelling Framework for Projections of Climate Change Impacts on Health" by Vicedo et al. [58]. Figure 1 illustrates the main processes and statistical analysis we performed for this study. Our statistical analysis involved four main steps, these steps are highlighted with different colours in the background of Figure 1 and described in the following paragraphs. In summary, we first used a regression model to obtain location-specific exposure-response association estimates, which were then pooled in a second stage using a meta-regression model. We pooled the estimates for ten subgroups which we generated by categorizing the mortality counts into two age groups (>65 and ≤ 65), stratifying by sex and the six main causes of death in Peru. Later, we re-predicted the location-specific estimates as the best linear unbiased predictions (BLUPs). Then, we used the BLUPs to quantify the temperature-related mortality for each Peruvian department.

First stage, location-specific temperature-mortality associations.

The temperature-mortality associations were derived from the first stage of the case time series small-area analysis approach. This methodology allowed us to model multiple provinces' information within each department by using the following regression model:

$$g\left[\mathcal{E}(\gamma_{it})\right] = \alpha_{i(k)} + f(x_{it}, \ell) + I(dow_{it}) \tag{1.1}$$

In equation 1.1, function g is applied to the expected value of γ_{it}, which indicates the daily mortality for each of the cases i (provinces). The intercepts of the model α_i vary across each stratum k. Each stratum was generated with information on year, month, and province. The function that defines the non-linear association between temperature and mortality is represented by $f(x_{it}, \ell)$. For the function $f(x_{it}, \ell)$, our exposure variable x was modelled using distributed lag non-linear models (DLNMs). Additionally, we controlled for the day of the week, this is indicated in the equation

by $I(dow_{it})$. Thus, the regression model 1.1 included three regression terms that allowed us to evaluate risks at each Peruvian department using the information of different cases, control for confounders and include the delayed effects of our exposure variable (daily mean temperature).

To model the temperature-lag-mortality association, we used the `crossbasis( )` function, which is part of the *dlnm* package [68] in R. For the cross-basis, we applied a natural spline function and set three knots at the 10th, 75th and 90th percentiles of the temperature distribution for each location. To account for the effects of heat and cold, we set a 21-day lag window (ℓ) as suggested by Gasparrini et al. [69]. The outcomes of the cross-basis and the regression model were reduced from the bi-dimensional exposure-lagged-mortality association to one-dimensional. To reduce the outcomes, we used the `crossreduce( )` function in R from the *dlnm* package [68]. From this, we obtained a set of diverse location-specific covariates and coefficient estimates that we used in the second stage. This part of the analysis was performed for each of the subgroups that we worked with.

Second stage, multivariate multilevel meta-analysis.

In the second stage, we pooled and later re-predicted the estimates previously obtained. We pooled the estimates of all departments to generate an overall exposure-response function at a national level. We also pooled the estimates for each of the previously described subgroups. To pool and re-predict the estimates, we used a multilevel multivariate meta-regression model as described by Sera et al. [70]. The formulation of the regression model used in this project is shown in equation 1.2.

$$y_j = X_j\beta + Z_j b_j + \epsilon_j \tag{1.2}$$

In the meta-regression model, the fixed effects are represented by $X_j\beta$, while the random effects are indicated by $Z_j b_j$. For this model, we used the mean and temperature range of each department j as meta-predictors. To include the geographical variability of the country, we grouped the Peruvian departments into 8 different areas and incorporated them into the model as random intercepts. The residual errors are denoted by ϵ_j. The analysis was performed using the `mixmeta( )` function in R, which is part of the *mixmeta* package [71]. To fit the model, we used the maximum likelihood estimation. After obtaining the pooled estimates with `mixmeta( )`,

we re-predicted them as the Best Linear Unbiased Predictors (BLUPs) using the `blup( )` function, which is also part of the *mixmeta* package [71]. The BLUPs are improved location-specific estimates that are generated by taking/borrowing information from different study locations [70, 72]. With the re-predicted estimates as BLUPs, we generated location-specific exposure-response curves. From the curves, we obtained the association between temperature and mortality expressed as the Relative Risk (RR) and we derived the Minimum Mortality Temperature (MMT) value for each department.

Quantification of the impact of non-optimal temperatures from 2009 to 2019.

To quantify the mortality burden due to non-optimal heat and cold, we first calculated the attributable number of deaths (AN) and then the attributable mortality fraction (AF) following the methodology of Gasparrini and Leone [73]. We derived the location-specific attributable number of deaths (AN) following the structure of equation 1.3.

$$AN = \sum_{d=1}^{n}((1 - \exp(-(\mathbf{C} * \beta)_d)) \cdot O_d) \tag{1.3}$$

Here, β represents the coefficients estimated as BLUPs for each location and O_d refers to the cumulative number of daily deaths. For the calculation, $\mathbf{C}$ was obtained by re-computing and deriving a centred basis for each department using as reference MMT. The value of MMT indicates the temperature at which the risk of death is the lowest and, it is also the reference point to define heat- and cold-related mortality. Days with a daily mean temperature lower than MMT are considered non-optimal cold temperatures. Conversely, non-optimal heat refers to days when the daily mean temperature is above MMT, potentially causing heat-related mortality.

To account for the imprecision of the temperature-mortality function, we quantified the uncertainty using Monte Carlo simulations. For this, we assumed a normal distribution of the point estimates and the covariates estimated as BLUPs. We performed 1000 Monte Carlo iterations to sample the estimates using the `mvrnorm( )` function in R, from the *MASS* package [74]. After, we summarized the results by computing the empirical confidence intervals at the 2.5th and 97th percentiles. Subsequently, we computed the proportion of attributable deaths in each department.

For this, we divided the location-specific attributable deaths by the total number of deaths that occurred in each department and multiplied the result by 100. We reported the attributable mortality fraction as a total, as well as separately for the heat and cold components.

Projection and quantification of the future impacts, from 2071 to 2099.

To quantify the future impacts, we followed the approach described by Vicedo et al. [58]. First, we extended the boundaries of the temperature-mortality curves for the departments of Ica, Madre de Dios and Ucayali. For this, we log-linearly extrapolated the exposure-response curves. Then, we used the *dlnm* package [68], specifically the `onebasis( )` function in R to represent the exposure-response as uni-dimensional. Afterwards, we predicted the overall Relative Risk (RR) with the extended range of simulated temperature values using the `crosspred( )` function in R, which is also part of the *dlnm* package [68]. Finally, we also quantified the future health impacts as attributable mortality fractions. The process was similar to the one described in the previous section. However, here we generated the estimates using the projected temperature values. And, we also used MMT to re-centre and transformed it to uni-dimensional with the `onebasis( )` function from the *dlnm* package [68]. Equation 1.4 illustrates the calculation of AN, which was later used to obtain the attributable mortality fraction (AF).

$$AN_f = \sum_{f=1}^{n}((1 - \exp(-(\mathbf{D} * \beta)_f)) \cdot d_f) \tag{1.4}$$

In equation 1.4, β_f represents the coefficients that were obtained as BLUPs in the second stage, and d_f indicates the future baseline mortality. After obtaining the projected attributable number of deaths, we computed the empirical confidence intervals, as described in the previous section. Here, to obtain the attributable fraction (AF), we divided the attributable number of deaths (AN) by the baseline mortality. We then summed the result and multiplied it by 29, the number of years projected for the temperature series (2071 to 2099). Finally, we multiplied by 100 the outcome of the previous division.

Chapter 2

Manuscript

As it was mentioned in Chapter 1, this thesis aimed to study the impacts of non-optimal temperatures on mortality in Peru under observed and future conditions. Although this master thesis also aimed to quantify the projected cold- and heat-related mortality fractions for 2071 to 2099, we only analysed three Peruvian departments due to the limitations in the spatial coverage of the future data. Therefore, we will submit for publication only the results from analysing the period from 2009 to 2019. This chapter presents our manuscript titled "Heat and cold-related mortality burden in Peru: a small-area analysis approach", which is to be submitted to the Environmental Epidemiology journal.

Heat and cold-related mortality burden in Peru: a small-area analysis approach.

Background: In recent years, the impact of non-optimal temperatures on excess mortality has been studied in different regions across the globe. However, Latin America is among the least researched regions, where few studies have quantified temperature-attributable mortality fractions. Although some studies have quantified temperature-related mortality in the biggest Peruvian cities, to date, a nationwide analysis has not been conducted yet. Here, we analysed the location-specific temperature-mortality associations at the department level and quantified cold and heat-related mortality fractions for the period 2009 to 2019.

Methods: We used an extended two-stage time series small-area analysis approach to analyse 1,156,601 deaths that occurred between 2009 and 2019 across all provinces

of Peru. In the first stage, we used a regression distributed lag non-linear model to obtain the association between temperature and mortality. Afterwards, the estimates from the first stage were pooled with a multilevel multivariate meta-regression model. Then, we re-predicted the estimates as the best linear unbiased predictors (BLUPs) and derived department-specific minimum mortality temperature (MMT) values. Lastly, we quantified the attributable mortality fraction due to non-optimal temperatures using MMT as our reference value.

Results: Our study illustrated that between 2009 and 2019, 8.77% [9% CI: 4.94% to 11.75%] of the total all-cause mortality in Peru was attributed to non-optimal temperatures. Cold-related mortality contributed the most to the excess mortality, with 8.16% [95% CI: 4.31% to 11.28%], while heat-related mortality accounted for 0.61% [95% CI: 0.38% to 0.85%]. We found that the mortality fraction linked to temperature was significantly higher for individuals aged 65 and older (11.38%) compared to the 4.64% observed in the population under 65 years old. The majority of the temperature-related mortality fractions were found in the departments of Puno, Junín and Huancavelica. Conversely, Loreto, Ucayali and Madre de Dios were the departments with the least excess mortality. The location-specific MMT varied from 15.1°C to 28.1°C, while the minimum mortality temperature percentile (MMP) varied from 84 to 99. However, these results were different when analysing all-cause mortality for individuals under 65 years old and for those aged 65 and above. Moreover, our study showed that nationwide exposure to extreme cold increased the relative mortality risk by 21.9% [95% CI: 11.7% to 33.1%] and by 8.6% [95% CI: 1.9% to 15.8%] for extreme heat.

Conclusions: Our results showed that most of the temperature-attributable mortality fraction was associated with non-optimal cold temperatures. Nevertheless, exposure to both extreme heat and cold increased the overall mortality risk. Although we did not find differences in temperature-mortality associations when analysing the male and female subgroups, our results indicate that the elderly population remains the most at risk. The majority of excess mortality was geographically distributed in departments located in higher altitudes and the southern part of the country, contrary to the areas with lower altitudes.

Keywords: temperature-related mortality, meta-analysis, cold-related, Peru

2.1 Background

Diverse authors have studied the association between mortality and non-optimal ambient temperatures [2, 9–12, 18]. This epidemiological research has become more relevant as extreme weather events, particularly heatwaves, have been increasingly linked to rising heat-related mortality [75–77]. By the end of the century, projections indicate that climate change will magnify heat-related mortality and morbidity [6]. However, current studies indicate that cold-related mortality accounts for most of the temperature-related excess mortality [2, 9, 11], which has been categorised as a significant global risk to human health [1].

Although the fraction of heat-related mortality is currently lower compared to deaths linked to cold temperatures, the impact of extreme heat on health does not have to be underestimated. In elderly individuals, high temperatures can worsen pre-existing health conditions [6]. In young infants, it can lead to a higher risk of mortality because their metabolism is still developing and their bodies cannot regulate temperature as easily [24, 41, 42]. Moreover, studies suggest that in the future, heat-related mortality could surpass and potentially outweigh cold-related mortality [6, 78]. Worldwide, extreme cold and heat-related mortality accounts for more than five million deaths per year [2]. Over fifty per cent of the excess temperature-related mortality occurs in Asia and Africa [2]. However, the impact of non-optimal high and low ambient temperatures has been quantified in only a few regions, with most studies focused on Europe and North America.

2.1.1 What this study adds

Latin American cities have grown faster since 1950 [79], making the region one of the most urbanized in the world [80]. It is estimated that by 2030, around 85 per cent of the Latin American population will live in urban areas, [81] and by 2050, Latin America and the Caribbean are projected to have 736.9 million inhabitants [5]. However, despite the large population at risk and the projected population increase, there are limited studies analysing temperature-related mortality in the region, as noted by Kephart et al. [13]. This research gap can be attributed to different factors, being the limited availability of mortality data one of the most significant. Access to datasets containing daily mortality counts for Latin America is difficult. To our knowledge, only the Multi-Country MultiCity (MCC) Collaborative Research Network and the Salud Urbana en América Latina (SALURBAL) projects have successfully compiled enough health data of the region to research the association

between temperature and mortality.

In 2021, Zhao et al. [2] studied 13 Latin American countries using the MMC dataset. Later, in 2022, Kephart et al. [13] analysed 326 cities of the region, employing information from the SALURBAL project. Zhao et al. [2] reported that in the region, over 160,000 deaths per year are cold-related, while approximately 36,000 are linked to extreme heat. These findings highlight the considerable extent of cold-related mortality, which was corroborated by the findings of Kephart et al. [13] that analysed 15,431,532 deaths.

Although Kephart et al. [13] analysed more cities where cold is predominant, their findings showed that between 2002 and 2015 5.09% [95% CI: 4.64% to 5.47%] of the total deaths were cold-related, while 0.67% [95% CI: 0.58% to 0.74%] were heat-related. Temperature-related mortality is significantly influenced by socioeconomic factors. However, only Bakhtsiyarava et al. [57] have investigated the impact of socioeconomic and demographic factors on temperature-related mortality in Latin America. These regional- and city-level studies have contributed significantly to quantifying the effect of non-optimal temperatures on mortality in Latin American countries. Nevertheless, to our knowledge, no comprehensive assessments have been conducted on temperature-mortality risks at the state level, covering all municipalities within each country.

To fill this research gap, we obtained daily mortality counts from the Ministry of Health of Peru (MINSA) for the years 2009 to 2019. We analysed them to quantify temperature-related mortality fractions at a department level using the small-area analysis approach developed by Gasparrini [59]. The small-area analysis approach aims to provide a localized and more accurate risk assessment by using small-scale data, which helps to reduce biases [59]. For our analysis, we aggregated the daily mortality counts at a province level, which we linked with daily mean temperatures obtained from the PISCOt v1.2 dataset provided by Huerta et al. [61].

2.2 Data & Methods

2.2.1 Study setting

Our project consisted of analysing 1,156,601 deaths recorded across all provinces of the country. Peru is organized into three levels of administrative divisions: departments, provinces, and districts. In this project, we focus on provinces and de-

partments, which are the second- and first-level administrative divisions. Provinces are subdivisions of the first-level administrative areas known as departments. Although in this project we refer to provinces as small areas, districts are the smallest administrative-level units in the country. We gathered all the geographic information and regional characteristics of the country from the Ministry of Environment of Peru (MINAM).

2.2.2 Data

We calculated the daily mean temperature for each province using high-resolution gridded data. We obtained the information from the PISCOt v1.2 dataset by Huerta et al. [61]. The dataset contains information on daily maximum and minimum temperatures for all of Peru from 1981 to 2020. PISCOt v1.2 provides data at spatial resolutions of 0.05° and 0.10°. For this project, we worked with the data available at 0.05° (approximately 5km) resolution.

We requested daily mortality counts from the Health Ministry of Peru (MINSA). The data provided included details on age, sex, International Classification of Diseases code for the cause of death [ICD-10], date of death, and the administrative division of each death. For estimating the pooled association between temperature and mortality, we categorized the data into distinct subgroups. These included all-cause mortality, all-cause fatalities among individuals aged 65 and older, those under 65, and both female and male groups. Additionally, we aggregated the information based on the six main causes of death across all population groups. We identified the main causes of death by the most frequent ICD codes, classifying each death into the relevant categories within the 22 chapters of the classification system. The most frequent categories included diseases of the circulatory system (I00 to I99), digestive system problems (K00 to K93), infectious and parasitic diseases (A00 to B99), neoplasms (C00 to D48), respiratory system diseases (J00 to J99) and external causes of morbidity and mortality (V01 to Y98).

2.2.3 Statistical analysis

We conducted all analyses with R (version 4.3.2) [82]. We followed an extended case two-stage time series small-area analysis as described by Gasparini [59]. In summary (Figure 1), we first linked daily mean temperature with daily mortality. Then, using a regression model (2.1), we obtained a set of estimates which later were pooled to obtain temperature-mortality associations for all-cause mortality,

as well as by age, sex and each main cause of death. Afterwards, we re-predicted the location-specific estimates as the best linear unbiased predictors (BLUPs) and derived the Minimum Mortality Temperature (MMT) for each department. Lastly, we quantified the location-specific temperature-related mortality.

Estimation of the exposure-response associations

To obtain the non-linear association between temperature and mortality in the first stage, we used the following regression model:

$$g\left[\mathcal{E}(\gamma_{it})\right] = \alpha_{i(k)} + f(x_{it}, \ell) + I(dow_{it}) \tag{2.1}$$

In the model, function g is applied to the expected value of $\mathcal{E}(\gamma_{it})$ that refers to the daily deaths for each of the cases i (provinces). Each of the intercepts of the model $\alpha_{i(k)}$ vary per stratum k across locations. Each stratum k was formed using information on the year, month and province where the death occurred. The function $f(x_{it}, \ell)$ defines the non-linear association between temperature and mortality. Our exposure variable x was modelled using Distributed Lag Non-linear Models (DLNMs). Here, we set a 21-day lag window (ℓ) to account for the delayed effects of cold and consider the shorter effects of heat as suggested by Gasparrini et al. [69]. Although some authors control for other confounder variables, we just controlled for the day of the week $I(dow_{it})$. We modelled the temperature-lag-mortality association by using the `crossbasis( )` function of the *dlnm* package [68] in R. For this, we used a natural spline function to account for the non-linearity and set 3 knots at the 10th, 75th, and 90th percentiles of the temperature distribution. The results obtained from the cross-basis were reduced to one-dimensional using the `crossreduce( )` function in R, which is also part of the *dlnm* package [68] in R.

After, in the second stage, we pooled the previously reduced estimates using a multilevel multivariate meta-regression model. This approach is further explained by Sera et al. [70]. By pooling the estimates, we combined the results from all locations to estimate an overall exposure-response function. We pooled the estimates for diverse subgroups which we obtained by classifying the mortality counts according to sex, age and cause of death. Because of the complex topography of Peru, we used three meta-predictors to improve our meta-regression. To account for the geographical differences between the departments, we aggregated them based on their

geographical similitude. This was incorporated into the model as random intercepts. Additionally, we included mean and range temperature as meta-predictors. For this analysis, we used the `mixmeta( )` function in R, which is part of the *mixmeta* package [71]. To re-predict the pooled estimates as the best linear unbiased predictors (BLUPs) we used the `blup( )` function that is also part of the *mixmeta* package [71]. Subsequently, we derived a new centred basis for the exposure-response function using the minimal mortality temperature (MMT) that was obtained from the BLUPs. MMT was obtained for each of the Peruvian departments, and it indicates the temperature at which mortality risk is the lowest and it is the reference value to define cold- and heat-related mortality. After re-centring, we computed the daily mortality contributions using the daily location-specific Relative Risk (RR).

Quantification of temperature-related mortality

We quantified temperature-related mortality, by calculating the attributable number of deaths (AN) and attributable fraction (AF%). To calculate the total attributable number of deaths (AN), we summed the total daily contributions calculated in the second-stage. Then, we aggregated them into two categories based on whether the temperature on the day of the death was below or above MMT. Cold-related mortality was determined by aggregating the deaths recorded on days when the mean temperature was lower than the MMT, while heat-related mortality was derived by estimating the number of deaths that occurred on days when the mean temperature was above the MMT value. Afterwards, we computed the total attributable fraction (AF%) for each department. For this, we divided the attributable number of deaths by the location-specific total mortality and then multiplied the result by 100. Finally, to account for the statistical uncertainty from the imprecision of the exposure-response function, we used Monte Carlo simulations to compute the empirical confidence intervals (eCIs) at the 2.5th and 97th percentiles. This methodology for deriving attributable risk from distributed lag models is further explained by Gasparini and Leone [73].

2.2.4 Sensitivity analysis

We tested the robustness of our analysis by conducting a sensitivity analysis. For this, we excluded the last three years of our study period and recalculated both the attributable number of deaths and the corresponding fractions, which we then compared with our main findings. Specifically, we omitted the years 2017, 2018 and 2019 to assess the impact of the introduction of the National Death Information

System (SINADEF) that was implemented in 2017 [83]. Additionally, to compare the 95% confidence intervals (CIs) of the exposure-response curves, we re-predicted the pooled estimates as BLUPs using the same modelling framework, but with the temperatures from the enhanced resolution reanalysis dataset ERA5-Land [84] instead of PISCOt v1.2 [61].

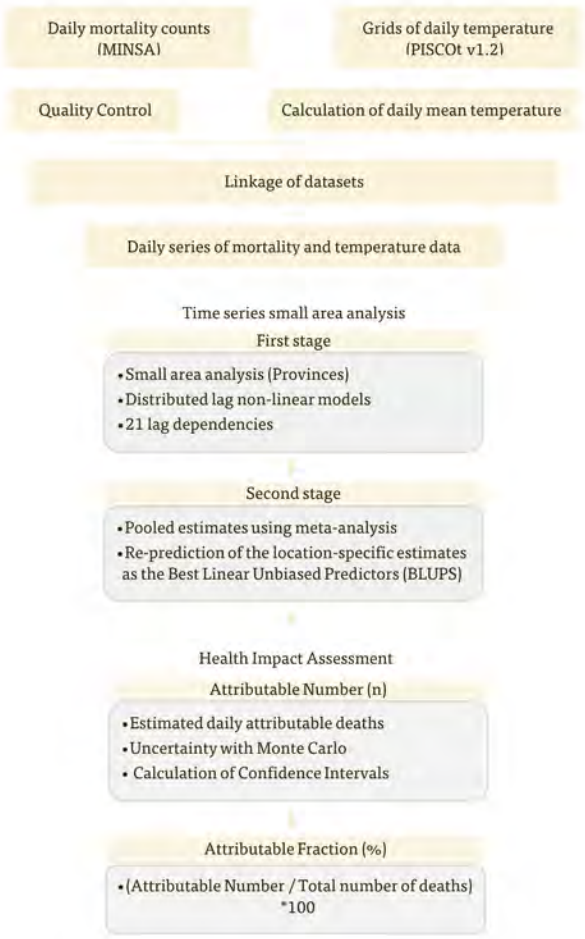

Figure 1: Modeling framework methodology. The flowchart describes the main three steps of the study approach used for this project.

2.3 Results

2.3.1 Descriptive statistics

Between 2009 and 2019, a total of 1,156,601 deaths were recorded across Peru. Supplementary Table S.1 provides a summary of the mortality data aggregated by department, including the range and mean temperatures calculated for each location.

The temperature range varied from 1.3°C to 12.7°C. Loreto, a department located in the rainforest region, had the highest mean temperature at 26.8°C, while Puno had the lowest at 8.6°C. Out of all the departments of the country, the Department of Lima recorded the highest number of deaths, while Madre de Dios registered the least. Of the total mortality counts, 53.49% were male, and 60.23% of the deaths occurred among individuals over 64 years old (See Table S.2 in the Supplementary Material). We categorized the total mortality counts into 22 groups corresponding to each chapter of the International Classification of Diseases (ICD-10), 2019 edition [85] (See Supplementary Table S.3). Out of the 22 categories, six accounted for 82.38% of the total deaths (Supplementary Table S.4).

2.3.2 Pooled temperature-mortality associations

Figure 2 illustrates the overall association between temperature and all-cause mortality over the study period (2009-2019).

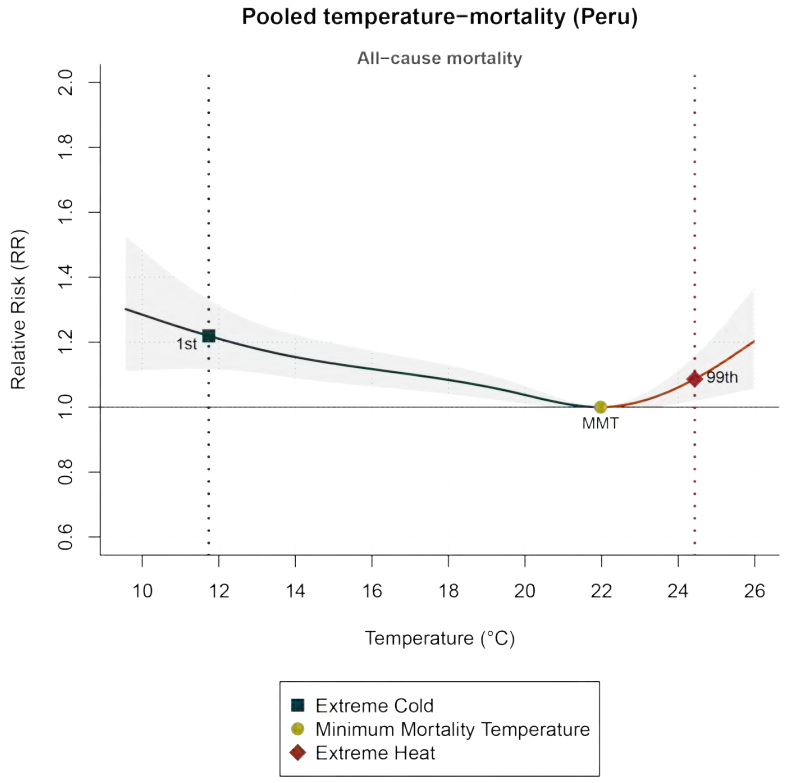

Figure 2: Overall exposure-response association for Peru. The temperature-mortality association for Peru was obtained by pooling the estimates from the first stage using a multi-parameter meta-analysis approach. Cold-related relative risks are indicated in blue, while heat-related risks are shown in red. The dotted vertical line in blue indicates the 1st percentile (extreme cold) and the red one shows the 99th percentile (extreme heat). The 95% CI is indicated in shaded grey.

The pooled curve shows a typical reverse J-shape, an MMT of 21.98 °C and an increasing mortality risk for both cold and hot temperatures. The left side of the curve, below the MMT, indicates the cold-related relative risks, while the right side illustrates the risks associated with hot temperatures. We defined extreme cold as the temperatures lower than the 1st percentile of the temperature distribution and extreme heat as temperatures higher than the 99th percentile. These are indicated by blue and red dotted lines in Figure 2. The overall population shows higher vulnerability to extreme cold, with an increased mortality risk of 21.9% [95% CI: 1.117 - 1.331], while extreme heat raises the risk by 8.6% [95% CI:1.019 - 1.158].

Figure 3a displays the pooled association between temperature and all-cause mortality for individuals younger than 65 years and those 65 years and older. Temperature-related risks for individuals under 65 years are shown in light green, while mortality risks for those aged 65 and older are represented by a darker green line. For individuals under 65 years old, the Minimum Mortality Temperature (MMT) is 20.29°C, while for those aged 65 and older, it is 21.98°C.

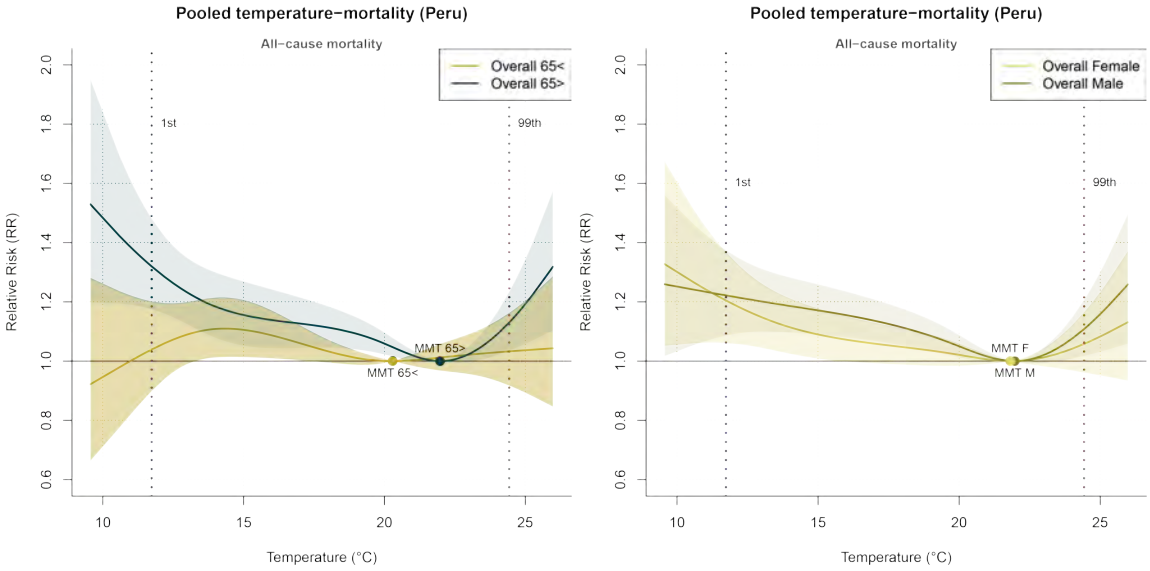

(a) Exposure-response association by age. **(b)** Exposure-response association by sex.

Figure 3: Pooled estimates of the overall temperature-mortality association by age and sex group. The exposure-response associations are shown for all-cause mortality. In both figures, the 1st percentile (extreme cold) is indicated by vertical blue dotted lines and in red for the 99th percentile (extreme heat).

For individuals aged 65 and older, the temperature-mortality association curve displays a reverse J-shape, indicating a higher mortality risk associated with colder

temperatures. Exposure to extreme cold increases the vulnerability of individuals aged 65 and older by 31.9% [95% CI:1.175 - 1.481], while exposure to extreme heat raises their risk by 13.1% [95% CI:1.035 - 1.234]. In comparison, for individuals below 65 years old, vulnerability to extreme cold increases by 3.9% [95% CI:0.899 - 1.201], and exposure to extreme heat raises their risk by 3.3% [95% CI:0.917 - 1.162].

Figure 3b illustrates the exposure-response association between temperature and mortality for the female and male subgroups. The mortality risk by sex shows minimal variation between the two groups. Both groups exhibit a higher relative risk associated with cold temperatures, with their Minimum Mortality Temperature (MMT) values being quite similar: 21.98°C for males and 21.81°C for females. Mortality risk to extreme cold increases similarly for both sexes. For females, the risk rises by 20.4% [95% CI:1.061 - 1.367], while for males, it increases by 22.2% [95% CI:1.086 - 1.374]. At the 99th percentile, which indicates extreme heat, vulnerability to mortality increases by 5.8% [95% CI:0.961 - 1.164] for females and by 10.8% [95% CI:1.018 - 1.207] for males.

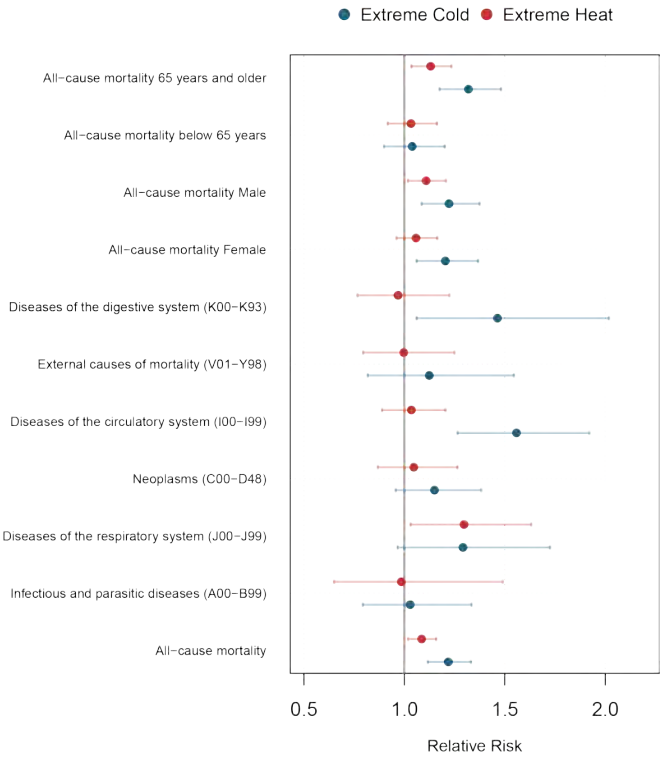

Figure 4: Pooled association estimates at the 1st and 99th percentiles for all-cause mortality, sex, age group and the main 6 causes of death in Peru (RR with 95% CI). The relative risks for extreme heat (99th percentile) are illustrated in red and in blue are indicated the ones for extreme cold (1st percentile).

Figure 4 presents a comparison of relative risks and 95% CIs for cause-specific mortality across extreme temperatures. Extreme cold-related risks are highest for digestive system diseases (RR = 1.463 [1.061 - 2.018]), circulatory problems (RR = 1.558 [1.265 - 1.92]), and respiratory issues (RR = 1.292 [0.967 - 1.725]). In contrast, heat-related relative risks are lower, particularly for digestive system diseases (RR = 0.969 [0.767 - 1.224]) and infectious and parasitic diseases (RR = 0.985 [0.651 - 1.489]). Supplementary Table S.5 provides a detailed breakdown of the results for each cause of death, including the estimated MMT. The overall exposure-response curves by each cause of death are illustrated in Supplementary Figure S.1. In summary, the curves for circulatory system diseases, neoplasms, and digestive system diseases show a reverse J-shaped relationship. This pattern indicates a higher mortality risk at colder temperatures.

2.3.3 Location-specific associations between temperature and all-cause mortality

Temperature-mortality associations were obtained for each of Peru's 25 departments. The exposure-response associations, estimated as best linear unbiased predictions (BLUPs), are illustrated in the Supplementary Figures S.2, S.3 and S.4. Most curves show either a J-shaped curve, which indicates increased mortality risk at both cold and hot extremes compared to moderate temperatures, or a reverse J-shape relationship, indicating higher mortality risk at colder temperatures with a relative decrease at warmer temperatures. However, the curves for Ancash, Apurímac, Ayacucho, Cusco, Huancavelica, Junín, and Puno display an L-shape pattern, illustrating a relatively constant risk across temperatures, with a notable increase only at extreme cold.

From the second stage, we obtained the Minimum Mortality Percentile (MMP) and Minimum Mortality Temperature (MMT). Using the location-specific exposure-response curves, we derived the MMT for each department. Figure 5 illustrates the geographical distribution of MMP and MMT across Peru. Figure 5a indicates that MMP values were higher in the southern departments of the country, while those in the northern region display lower percentile values. Specifically, the highest MMP values were found for the departments of Puno, Junín, Huancavelica, Ayacucho and Apurímac, which reached up to the 99th percentile threshold. In contrast, Lambayeque, Amazonas, Pasco and Piura showed the lowest MMP values.

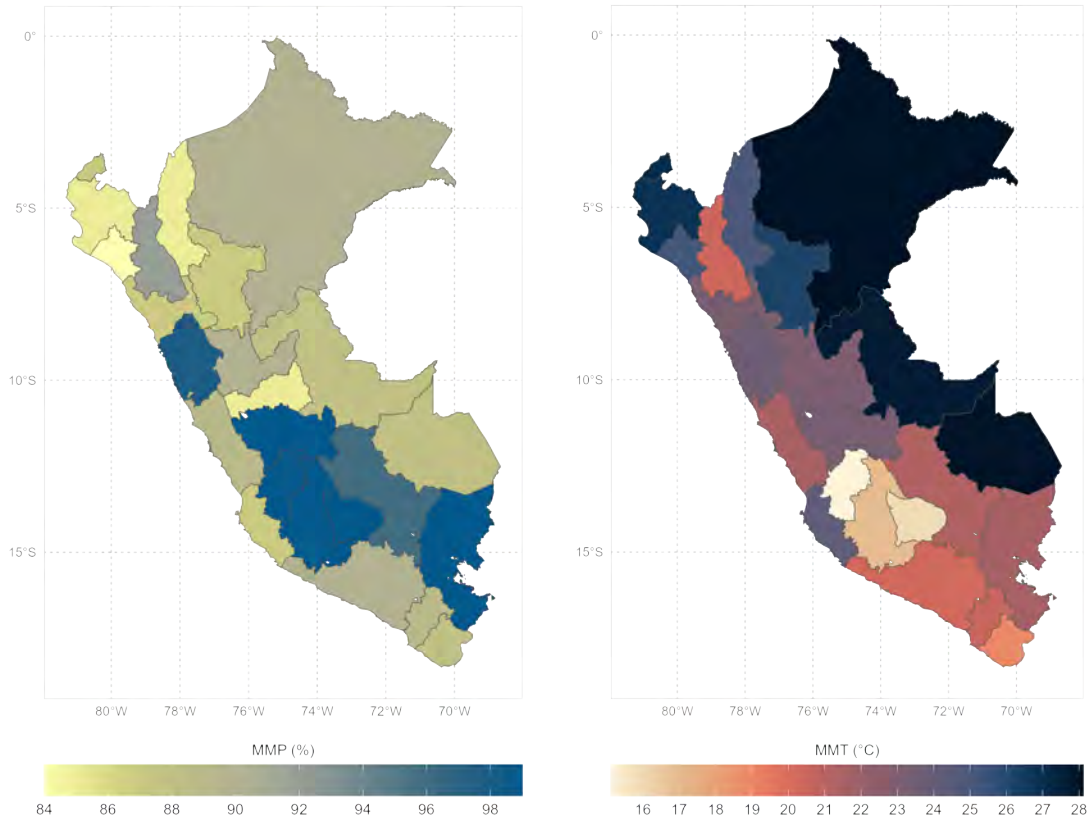

(a) Minimum Mortality Percentile (%) **(b)** Minimum Mortality Temperature (°C)

Figure 5: Nationwide geographical distribution of the Minimum Mortality Temperature (MMT) and Minimum Mortality Percentile (MMP). The maps show the distribution of MMT and MMP across all of Peru's departments.

Figure 5b displays the spatial distribution of MMT. Contrary to the MMP geographical distribution, the highest MMT values are distributed in the northern region of the country, while the lowest MMT values are observed in the southern departments, specifically in Huancavelica, Apurímac and Ayacucho. The MMT values range from 15.13 °C to 28.11 °C, these location-specific MMT values are presented in Supplementary Table S.6. The values of MMT, along with their respective MMPs, are displayed for each department, including both the population groups under 65 years old and individuals aged 65 and older.

Figure 6 shows the mortality risks to extreme heat and cold. Most of the heat-related Relative Risks (RRs) were greater in departments situated along the coast and in areas with lower elevations. Our findings showed that exposure to extreme heat did not present an increased risk for the following departments: Ayacucho, Ancash, Junín, Puno, Apurímac, Huancavelica, and Cusco (See Supplementary Table S.7 and Sup-

plementary Figure S.5). However, exposure to extreme heat significantly increased the vulnerability for Lambayeque (19.2%), Pasco (18.9%) and Callao (18.3%).

In comparison, exposure to extreme cold temperatures was found to increase mortality risk (RR) the most for the departments of Apurímac (35.2%), Huancavelica (35.8%), Junín (35.9%) and Puno (52.7%). Conversely, Loreto (7.9%), Ucayali (8.9%) and Madre de Dios (10.6%) showed less vulnerability to extreme cold temperatures. For further details, see Supplementary Table S.7 and Supplementary Figure S.5. Figure S.5 illustrates the Relative Risks (RRs) for extreme heat and cold across all Peruvian departments. In Table S.7 we present the Relative Risks (RRs) with their 95% CIs for exposure to moderate and extreme temperatures across all departments.

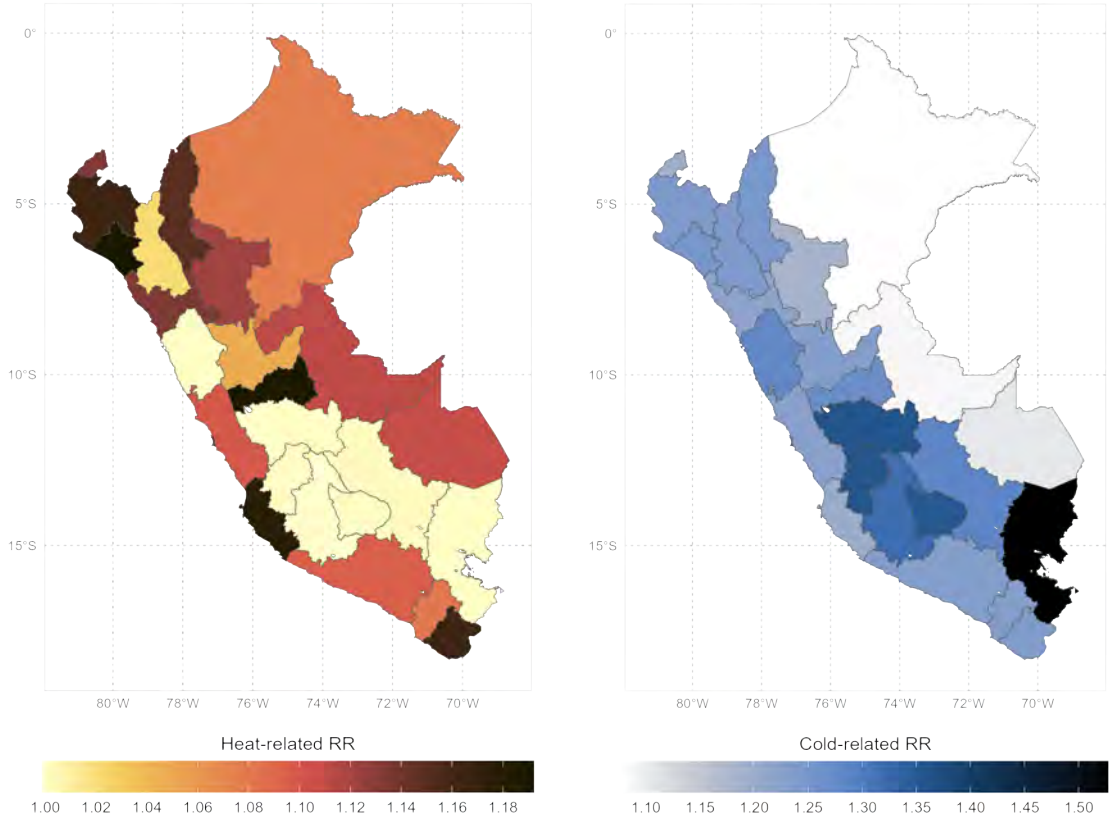

(a) Extreme heat-related RR **(b)** Extreme cold-related RR

Figure 6: Geographical distribution of the relative risks linked to extreme heat and extreme cold. The maps illustrate the relative risks (RR with 95%CI) to extreme heat (99th percentile) and extreme cold (1st percentile) across Peru.

2.3.4 Mortality fraction attributed to non-optimal temperatures

We computed the mortality fraction attributed to non-optimal temperatures for each department using the location-specific MMT values as the reference for optimal temperature. First, we obtained the heat- and cold-related number of deaths, which we used to calculate the location-specific attributable fractions. These results are reported in the Supplementary material for each department. Table S.8 displays the all-cause mortality estimates, Table S.9 presents the attributable number of deaths (AN) for the population under 65 years old, and Table S.10 shows the AN for the individuals aged 65 and older. In the tables, we report the AN as a total and for both, the heat and cold component, this allowed us to compute the heat- and cold-related attributable fractions. The cold-related fraction refers to the proportion of mortality that occurred when the mean temperature was lower than the MMT value, while the heat-related fraction describes the proportion of mortality occurring when the mean temperature exceeded the MMT. The calculation of these fractions for each Peruvian department are presented in Table 1. Additionally, the attributable fractions for the population groups under 65 years old and those aged 65 and older are presented in Tables S.11 and S.12, respectively.

Table 1: Estimated mortality fraction attributable to non-optimal temperatures between 2009 to 2019 by department. The 95% CIs are displayed in square brackets.

	Attributable Fraction (%)		
Department	**Total**	**Cold**	**Heat**
Amazonas	8.24 [2.24 : 13.22]	8.04 [2.09 : 13.03]	0.20 [0.09 : 0.32]
Ancash	10.28 [-2.57 : 20.33]	10.28 [-2.59 : 20.37]	0.00 [-0.04 : 0.04]
Apurímac	14.18 [-0.30 : 26.01]	14.19 [-0.29 : 26.05]	-0.01 [-0.05 : 0.03]
Arequipa	13.58 [7.76 : 18.85]	13.49 [7.62 : 18.73]	0.09 [0.03 : 0.16]
Ayacucho	13.93 [0.85 : 24.91]	13.94 [0.85 : 24.97]	-0.01 [-0.05 : 0.03]
Cajamarca	9.74 [3.27 : 15.31]	9.69 [3.19 : 15.29]	0.05 [-0.19 : 0.28]
Callao	8.10 [5.04 : 11.26]	7.40 [4.37 : 10.53]	0.70 [0.39 : 1.02]
Cusco	14.39 [4.37 : 22.91]	14.38 [4.31 : 23.02]	0.01 [-0.18 : 0.20]
Huancavelica	17.22 [1.84 : 29.95]	17.23 [1.84 : 30.02]	-0.01 [-0.06 : 0.04]
Huánuco	9.76 [4.09 : 14.69]	9.72 [4.03 : 14.70]	0.05 [-0.07 : 0.16]
Ica	7.09 [4.03 : 10.16]	6.18 [3.30 : 9.20]	0.92 [0.47 : 1.37]
Junín	20.03 [1.09 : 34.58]	20.04 [1.08 : 34.58]	0.00 [-0.01 : 0.01]
La Libertad	5.19 [2.99 : 7.18]	4.72 [2.52 : 6.76]	0.47 [0.26 : 0.67]
Lambayeque	4.53 [1.83 : 7.29]	3.47 [0.92 : 6.08]	1.07 [0.49 : 1.66]
Lima	4.96 [3.04 : 6.69]	3.88 [2.13 : 5.51]	1.08 [0.46 : 1.69]
Loreto	2.32 [-3.73 : 8.20]	2.13 [-4.04 : 8.12]	0.19 [-0.05 : 0.43]
Madre de Dios	2.59 [-2.70 : 7.25]	2.03 [-3.23 : 6.94]	0.56 [-0.07 : 1.16]
Moquegua	10.39 [6.49 : 14.22]	10.01 [6.05 : 13.80]	0.38 [0.04 : 0.72]
Pasco	14.33 [-17.00 : 33.69]	13.78 [-17.27 : 33.18]	0.55 [-0.10 : 1.17]
Piura	4.37 [1.10 : 7.78]	3.48 [0.14 : 6.83]	0.89 [0.39 : 1.37]
Puno	28.18 [4.42 : 46.04]	28.18 [4.41 : 46.05]	0.00 [-0.02 : 0.01]
San Martín	4.30 [1.00 : 7.49]	3.38 [0.33 : 6.52]	0.92 [0.32 : 1.54]
Tacna	7.69 [2.44 : 12.36]	7.56 [2.29 : 12.21]	0.13 [-0.07 : 0.33]
Tumbes	3.62 [-1.28 : 8.58]	3.26 [-1.74 : 8.16]	0.36 [0.05 : 0.67]
Ucayali	2.48 [-3.59 : 8.05]	2.21 [-3.94 : 7.82]	0.28 [-0.05 : 0.59]

Table 1 shows that the highest overall mortality fractions occured in the departments of Puno, Junín, Huancavelica, Cusco, Apurímac and Pasco, with a significant proportion attributed to cold temperatures. Specifically, the largest cold-related mortality fractions are reported for Puno, Junín and Huancavelica, while the departments of Madre de Dios, Loreto and Ucayali show the lowest proportions. These high overall and cold-related mortality fractions are found in departments located at higher elevations and the southern part of Peru, this pattern is illustrated in Figure 7.

Figure 7 shows the nationwide spatial distribution of the estimated mortality attributable fractions. Figure 7a illustrates the overall fraction, while Figure 7b and Figure 7c display the fractions related to cold and heat, respectively. Contrary to the pattern observed in Figure 7b, Figure 7c indicates that the highest mortality fractions attributable to heat are distributed in departments located in the northern and coastal areas of Peru. The highest heat-related mortality fractions are observed in the departments of Lima, Lambayeque and San Martín . However, no heat-related mortality fractions are reported for the departments of Huancavelica, Apurímac, Ayacucho, Puno, Junín and Ancash.

At the national level, we estimated an overall attributable mortality fraction of 8.77% [95% CI:4.94% to 11.75%] for our study period. Most of this fraction was attributed to cold temperatures, which accounted for 8.16% [95% CI: 4.31% to 11.28%]. In contrast, non-optimal heat accounted for 0.61% [95% CI: 0.38% to 0.85%] of the total fraction. For individuals under 65 years old, non-optimal temperatures were estimated to contribute for 4.64% [95% CI: 1.69% to 6.64%] of the total mortality. Specifically, non-optimal cold temperatures contributed 4.34% [95% CI:0.82% to 7.02%], while non-optimal heat accounted for 0.30% [95% CI:-0.61% to 1.12%]. In comparison, for individuals aged 65 and older, we estimated that cold accounted for 10.42% [95% CI: 4.75% to 15.22%] of the total mortality fraction, while 0.95% [95% CI: 0.55% to 1.34%] was related to non-optimal heat.

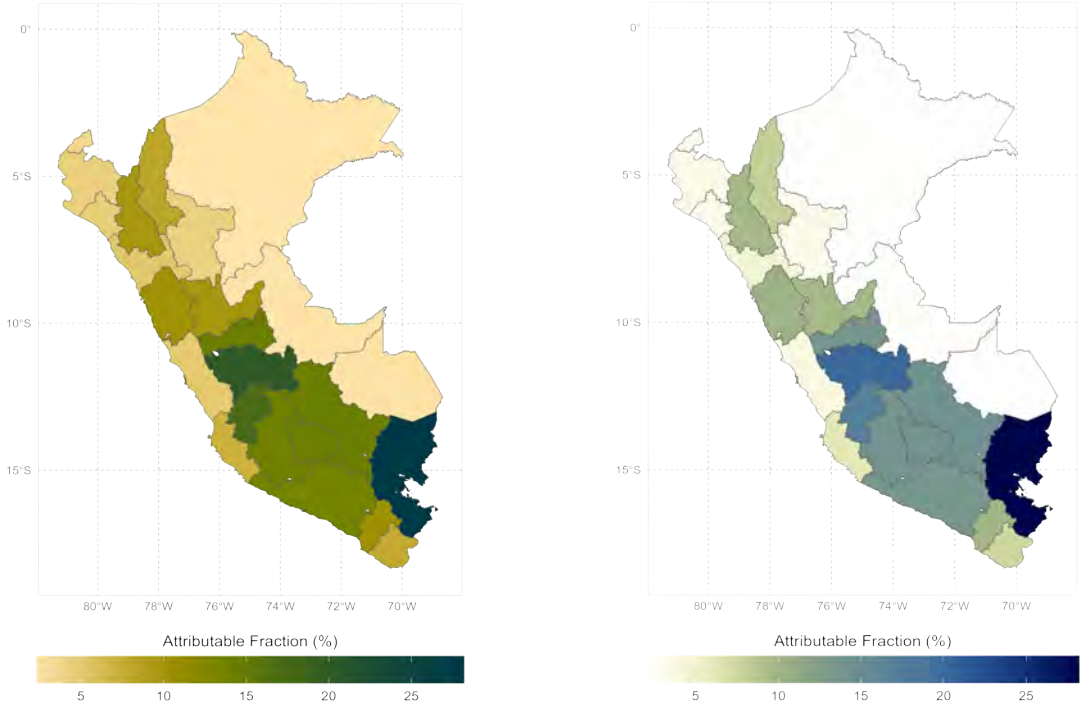

(a) Overall mortality

(b) Cold-related mortality

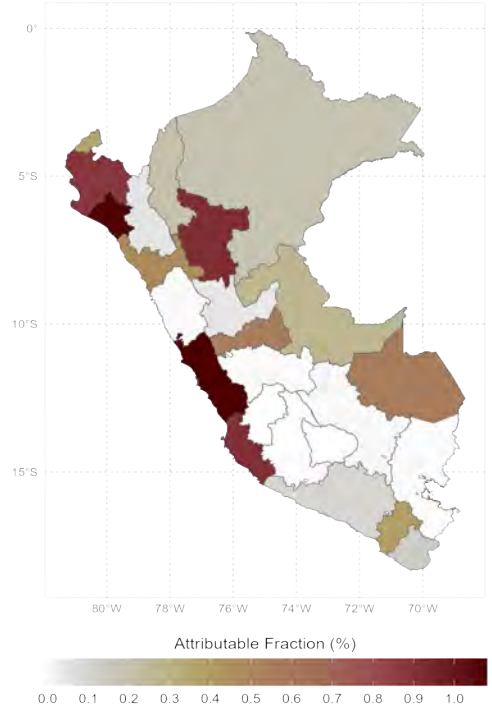

(c) Heat-related mortality

Figure 7: Geographical distribution of the attributable all-cause mortality fraction (AF%) to non-optimal temperatures. The maps illustrate the computed mortality fraction attributed to non-optimal temperatures in Peru between 2009 and 2019 for all age groups. The results are displayed in three separate figures that correspond to the overall mortality and individually for heat and cold.

2.4 Discussion

In this project, we analyzed 1,156,601 all-cause mortality deaths which were recorded from 2009 to 2019 across all departments in Peru. Our findings showed that non-optimal temperatures accounted for 8.77% of the total all-cause mortality. Most of the nationwide temperature-related mortality was linked to cold temperatures. We observed that for individuals aged 65 years and older, the overall proportion of mortality associated with non-optimal temperatures was 11.38%, which was higher compared to the 4.64% observed in the population below 65 years. Nevertheless, in both population groups, cold-related mortality accounted for most of the burden.

Studies using a similar approach to ours have also found a higher burden of cold in temperature-related mortality [2], [13], [14], [9]. For instance, Zhao et al. [2] estimated that for Latin America and the Caribbean, 200,055 (95% CI: 181,608 to 227,270) deaths per year can be linked to non-optimal temperatures. Specifically, 163,360 (95% CI: 134,007 to 194,240) deaths every year are associated with cold temperatures, while 36,695 fatalities (95% CI: 20,064 to 59,526) are heat-related [2]. In comparison, Kephart et al. [13], who analysed city-specific temperature-mortality associations for 326 Latin American cities, also reported higher mortality fractions due to non-optimal cold temperatures. For Peru, Kephart et al. [13] analysed the cities of Arequipa, Ayacucho, Cajamarca, Chiclayo, Chimbote, Chincha Alta, Cusco, Huancayo, Huaraz, Huánuco, Ica, Iquitos, Juliaca, Lima, Pisco, Piura, Pucallpa, Puno, Sullana, Tacna, Tarapoto, Trujillo and Tumbes. Their findings showed that from 2008 to 2015, cold-related mortality was the highest among the cities of Huaraz, Cajamarca and Puno with rates of 77.6%, 64.1% and 30.7% respectively [13, Supplementary Material]. Conversely, the study indicates that mortality in the cities of Tacna, Cusco, Tarapoto, Tumbes, Huancayo, Trujillo and Huánuco was not linked to non-optimal cold temperatures [13, Supplementary Material].

Even though the outcomes from Kephart et al. [13] are not fully comparable with our results due to differences in spatial scales, there are some similarities between the findings. Our findings indicated that the highest mortality fraction due to cold was observed in the department of Puno at 28.18%, similar to the 30.7% reported by Kephart et al. [13, Supplementary Material]. Additionally, Kephart et al. [13] estimated an MMT of 21.1 °C for the city of Lima, while our estimate for the department of Lima was 21.5 °C, which is very alike. Moreover, we obtained an MMT value of 19.0 °C for the department of Tacna, whereas Kephart et al. [13] estimated an MMT of 19.3 °C for the capital city of the same name, which is also

similar.

We found that heat-related mortality accounted for 0.6% of total deaths during our study period. Our estimates showed that the highest mortality fractions related to heat occurred in the departments of Lima, Lambayeque, Piura and Ica (See Table 1). In comparison, Kephart et al. [13, Supplementary Material] reported higher heat-related mortality fractions in the cities of Iquitos, Pucallpa and Chincha Alta, which are located in the departments of Loreto, Ucayali and Ica. Both our results and those of Kephart et al. [13] showed that heat-related mortality fractions are higher in geographic areas with lower altitudes. Furthermore, neither study found any heat-related mortality in the departments of Puno, Junín, and Ancash during their respective study periods.

Although Kephart et al. [13] and our study found that heat contributed the least to temperature-related mortality, extreme heat-related outcomes should not be underestimated. Vicedo et al. [16], who assessed the impact of heat and climate change on mortality in diverse regions of the world, reported that 73.5% of the heat-related Peruvian deaths can be attributed to anthropogenic climate change. This estimation was obtained using mortality data provided by the MCC Collaborative Research Network, which included 208,060 deaths across 18 Peruvian departments during the four warmest consecutive months at each location. The findings of Vicedo et al. [16, Supplementary Material] showed that Puno, Lima, Arequipa and Loreto were the departments with the highest fraction of heat-related mortality attributed to anthropogenic climate change, with 86.8%, 81.4%, 80.2% and 80%, respectively. In contrast, Huancavelica, Ayacucho and Apurímac were reported to experienced the least heat-related mortality per year due to human-induced climate change [16, Supplementary Material].

Vicedo et al. [16] found that the highest heat-related mortality fractions attributable to anthropogenic climate change occurred in the departments of Loreto, La Libertad and Lambayeque. This differs from our results, which indicated higher heat-related mortality in the departments of Lima, Lambayeque and Ica. Additionally, Vicedo et al. [16] reported the lowest heat-related mortality fractions due to anthropogenic climate change for the departments of Huancavelica, Ayacucho and Junín, which is similar to our findings that indicated the absence of heat-related mortality in the departments of Huancavelica, Ayacucho, Apurímac, Junín, Puno, and Ancash. However, regardless of the similarities and differences between our findings and those reported by Vicedo et al. [16], direct comparison is not possible because of the

different approaches used in each study. For our project, we used a 21-day lag for the regression model and included data from all months of the year to account for the effects of cold and heat, as recommended by Gasparini et al. [69]. In contrast, Vicedo et al. [16] analysed the deaths that occurred during the four warmest months at each location and applied a 10-day lag window to study the effects of extreme heat. Moreover, their analysis included two scenarios: the assessment of both natural and anthropogenic climate change.

In our pooled results, stratified by subgroups based on age, sex and cause of death, we found similar mortality risk (RR) and MMT for both male and female groups, with only minimal variations. However, we found that exposure to extreme cold temperatures increased the vulnerability by 31.9% for individuals aged 65 and older, whereas for those under 65 years, the increase was 3.9%. Additionally, extreme heat was associated with a 3.3% increase in mortality risk for individuals under 65 years old, while for the population aged 65 and older, extreme heat exposure showed an increase of 13.1%. These findings align with diverse studies that have reported the high vulnerability of elderly populations to non-optimal temperatures. For instance, Kephart et al. [13] found that the Latin American individuals aged 65 years old and older are more vulnerable to non-optimal temperatures, as well as Vicedo et al. [86] reported that elderly women are affected the most by non-optimal heat. However, in this study we did not investigate the combined effects of age and sex on vulnerability. Lastly, we found that mortality risk (RR) increases significantly for circulatory system and digestive diseases with exposure to extreme cold temperatures. These findings are consistent with the results reported by Kephart et al. [13], who found higher mortality fractions associated to extreme cold for cardiovascular diseases across Latin American cities.

2.4.1 Strengths and limitations of the study

Our study has diverse strengths. To date and to our knowledge this study is the first to provide a nationwide perspective on the effects of non-optimal ambient temperatures across all Peruvian departments. Here, we use high-resolution temperature data (0.05°) and daily mortality aggregated by provinces. Our study illustrates the robust association between temperature and mortality for the six leading causes of death in Peru. Additionally, we demonstrate the increased vulnerability of elderly individuals to extreme temperatures. Finally, we provide robust location-specific estimates of temperature-related mortality fractions for both heat and cold compo-

nents. These results are provided as an overall accounting for all ages, as well as for two subgroups: individuals aged 65 years and older and those below 65 years.

Nonetheless, we acknowledge the limitations of our study that should be addressed in future research. Our statistical model did not control for other exposure variables such as air pollution and humidity. Some studies have reported that high concentrations of air pollution modify the impact of higher temperatures on mortality [87–89]. Specifically, higher concentrations of air pollutants like PM_{10}, $PM_{2.5}$, O_3 and NO_2 can modify cardiovascular and respiratory mortality [90]. For instance, in the city of Lima, rising air temperatures have been reported to amplify the effects of $PM_{2.5}$ on mortality risk [91], and non-optimal $PM_{2.5}$ levels have been found to exacerbate the impact of temperature on birth weight [92].

While the effect of humidity on temperature-related mortality has not yet been studied in Latin America, it has been analysed in different regions [93–95]. A recent study focused on central China has found that higher humidity could potentially enhance cold-related mortality [93] while another study reported an increased morbidity risk due to humid heat in Shanghai [94]. Therefore, further analyses including humidity and air pollution could potentially influence our results. However, to date, there is no scientific consensus on the extent to which humidity and air pollution can impact temperature-related mortality. Moreover, we did not account for possible biases due to demographic and socioeconomic factors, which are significant drivers given that Latin America is one of the regions with the highest levels of inequality [96].

2.5 Conclusion

Altogether, our project provides robust information about excess mortality due to non-optimal ambient temperatures in Peru, highlighting both cold- and heat-related mortality fractions. Specifically, it presents estimates for each Peruvian department, considering the total population as well as two distinct age groups: individuals under 65 years and those aged 65 years and above. Our study indicates that, at the national level, exposure of the Peruvian population to extreme cold from 2009 to 2019 increased their risk of mortality by 21.9%, while extreme heat raised it by 8.6%. Additionally, we found that most of the mortality fraction attributed to non-optimal temperatures was geographically distributed among the southern departments of Peru. Finally, our project illustrates the potential number of Peruvian deaths that could have been avoided if proper adaptation measures and public health policies

were implemented in different departments.

2.6 Acknowledgments

No funding was received for conducting this study. However, Katia K. Hidalgo Olvera was partially supported by CONACYT Mexico during the first two years of her master's studies. Additionally, we acknowledge the cooperation of the Health Ministry of Peru in providing the recorded mortality datasets for the project.

2.7 Author Contributions

- Conceptualization: Katia K. Hidalgo Olvera, Ana María Vicedo Cabrera, Santos J. González Rojí, Martina Messmer and Adrian Huerta
- Study design and methodology: Katia K. Hidalgo Olvera, Ana María Vicedo Cabrera, Coral Salvador Gimeno and Evan De Schrijver
- Climate data: Adrian Huerta
- Mortality data resources and curation of climate and health datasets: Katia K. Hidalgo Olvera
- Formal analysis and visualization: Katia K. Hidalgo Olvera
- Project supervision: Ana María Vicedo Cabrera, Coral Salvador Gimeno and Evan De Schrijver
- Writing-original draft: Katia K. Hidalgo Olvera
- Writing-revision and editing: Katia K. Hidalgo Olvera, Coral Salvador Gimeno, Ana María Vicedo Cabrera, Santos J. González Rojí and Adrian Huerta.

2.8 Data Availability

Daily mortality counts were provided by the Health Ministry of Peru (MINSA). This data cannot be shared by the authors and should be requested directly from the Ministry. Series of high-resolution daily temperatures are public and available in the following repository: https://doi.org/10.6084/m9.figshare.c.5959863.v3. More detailed information can be found in the peer-reviewed publication: "High-resolution

grids of daily air temperature for Peru - the new PISCOt v1.2 dataset" by Huerta et al. [61]. Geospatial data and information on the administrative divisions of Peru were gathered from public sources of the government of Peru.

- The second and first administrative- divisions of Peru were obtained from the public website: https://www.idep.gob.pe/geovisor/descarga/visor.html
- We consulted the regional characteristics of the country at the official website of the Ministry of Environment of Peru (MINAM). The information was downloaded from https://geoservidor.minam.gob.pe/

To partially replicate the analysis, the first author of this paper has uploaded the R codes to the following repository: https://github.com/katiahidalgo/Non-optimal-temperatures-Peru.git.

2.9 Additional Information

We declare no competing interests.

2.10 Supplementary Figures

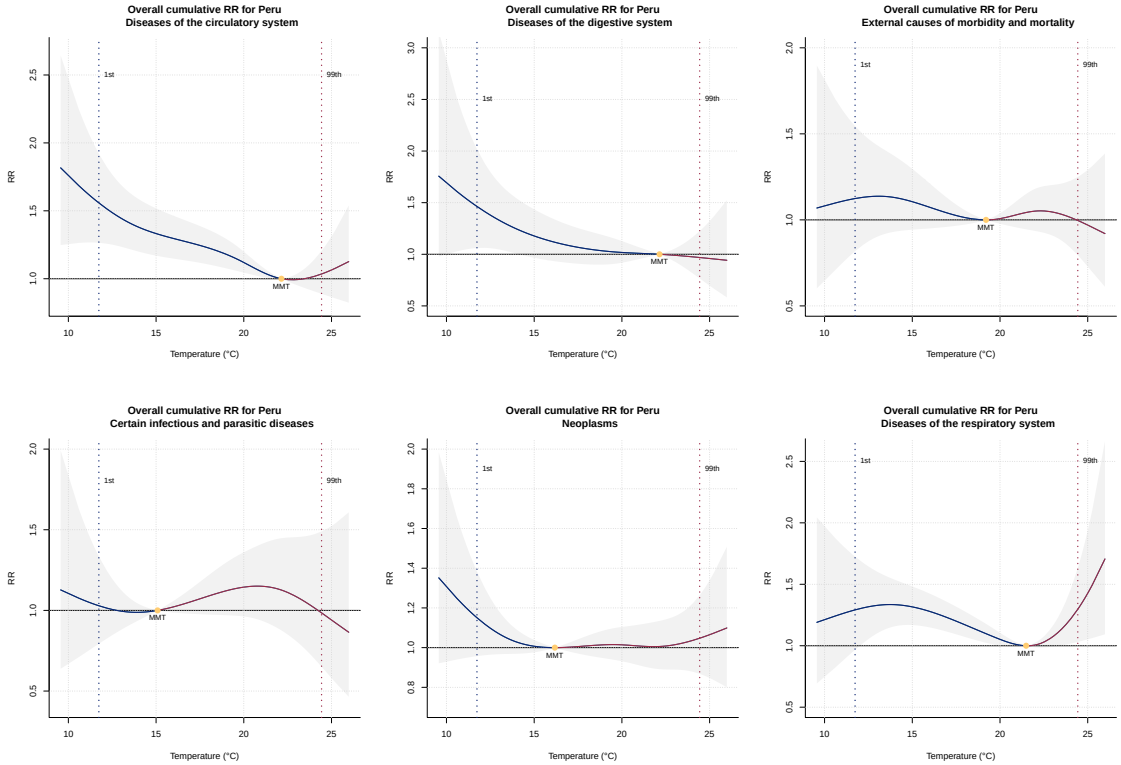

Figure S.1: Pooled estimates of the overall temperature-mortality association by the main 6 causes of death in Peru. The exposure-response associations are shown for the ICD codes J00-J99, C00-D48, I00-I99, V01-Y98, A00-B99 and K00-K93. In all figures, the 1st percentile (extreme cold) is indicated by blue dotted lines and in red for the 99th percentile (extreme heat).

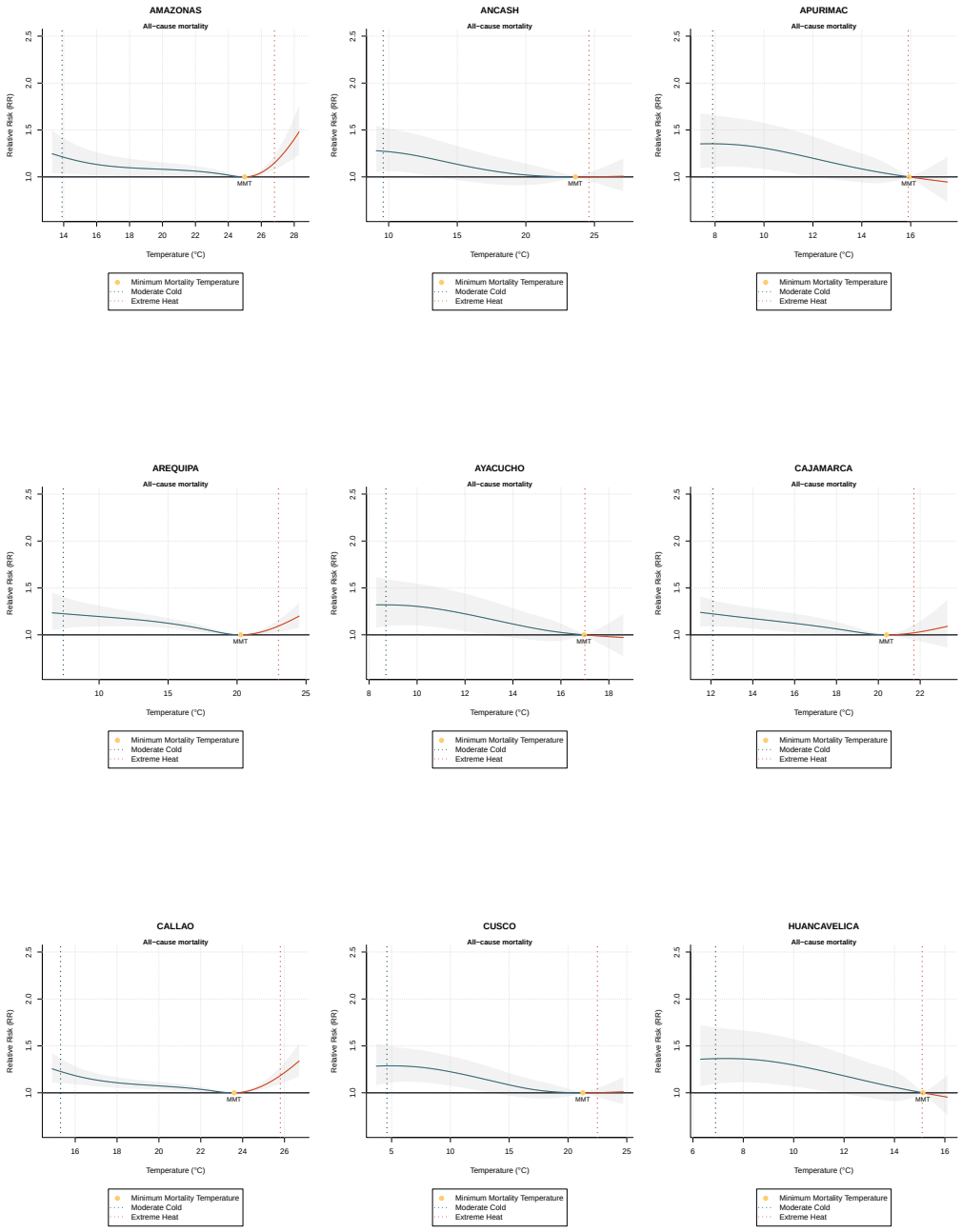

Figure S.2: Temperature-mortality associations estimated as the best linear unbiased predictions (BLUPs) over 21d lags for the departments of Amazonas, Ancash, Apurímac, Arequipa, Ayacucho, Cajamarca, Callao, Cusco, and Huancavelica. The relative risks of mortality (RR with 95% CI) were obtained for each department. We indicate the 99th percentile (extreme heat) with red dotted lines, and with blue ones, we illustrate the 2.5th percentile (moderate cold).

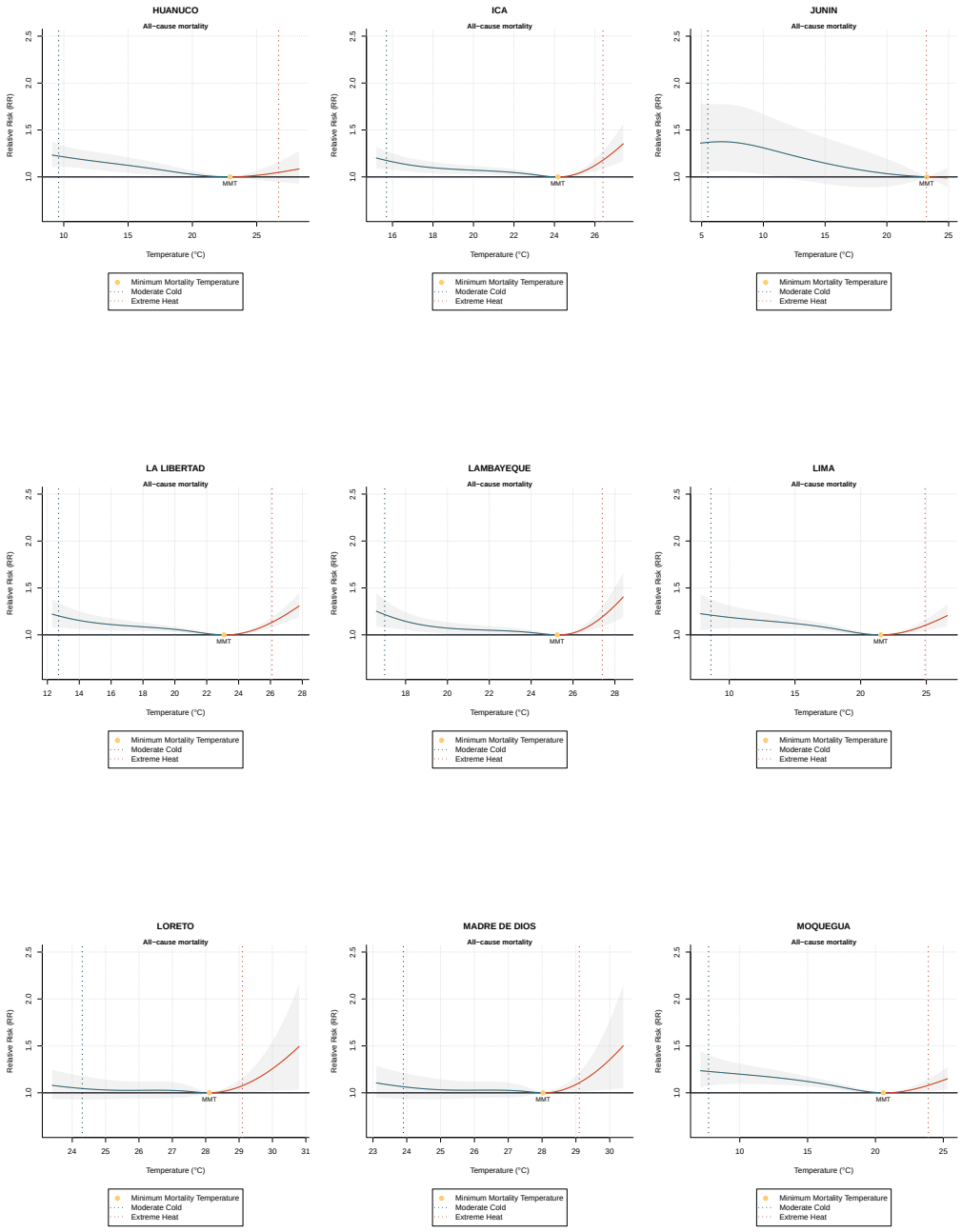

Figure S.3: Temperature-mortality associations estimated as the best linear unbiased predictions (BLUPs) over 21d lags for the departments of Huánuco, Ica, Junín, La Libertad, Lambayeque, Lima, Loreto, Madre de Dios, and Moquegua. The relative risks of mortality (RR with 95% CI) were obtained for each department. We indicate the 99th percentile (extreme heat) with red dotted lines, and with blue ones, we illustrate the 2.5th percentile (moderate cold).

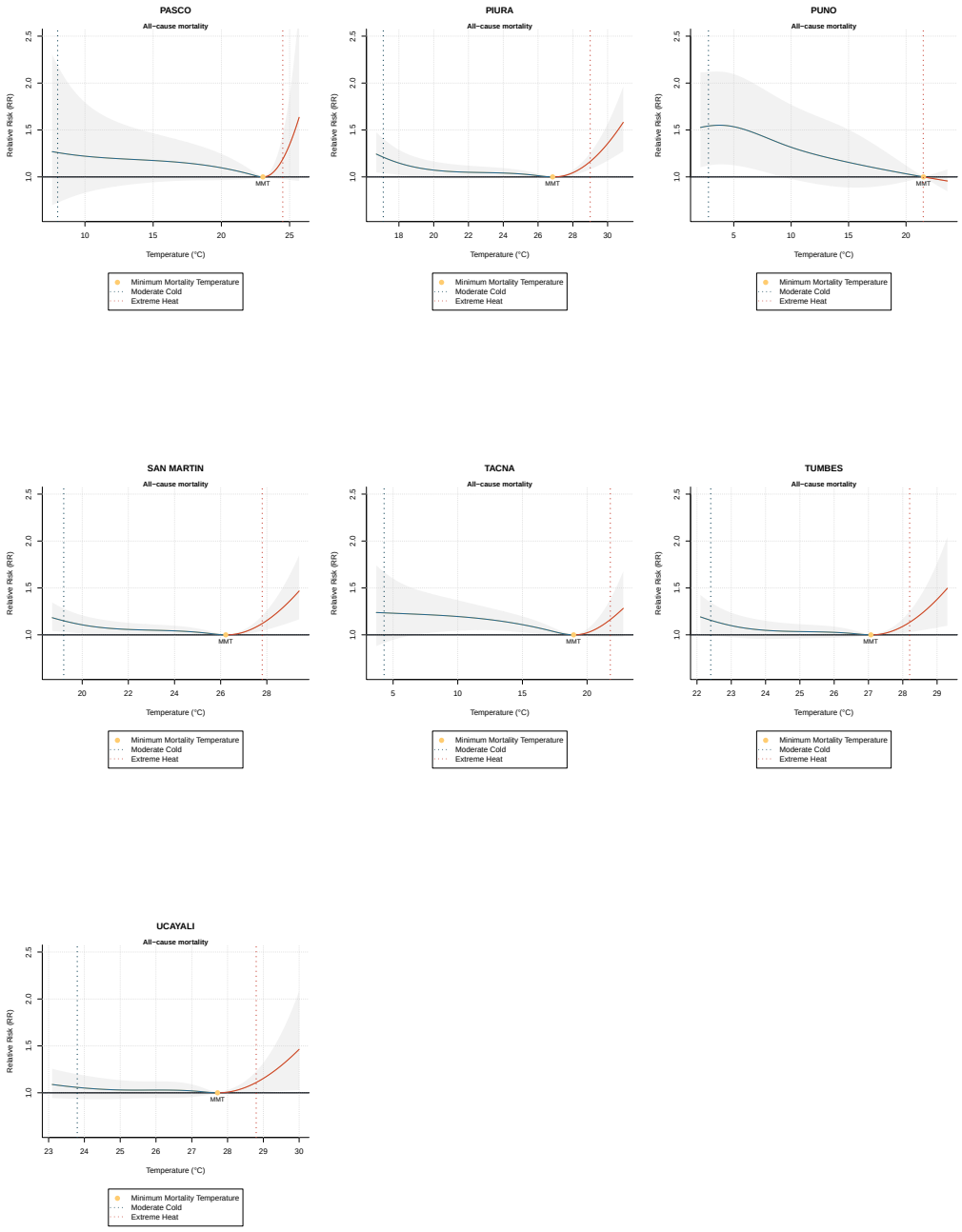

Figure S.4: Temperature-mortality associations estimated as the best linear unbiased predictions (BLUPs) over 21d lags for the departments of Pasco, Piura, Puno, San Martín, Tacna, Tumbes, and Ucayali. The relative risks of mortality (RR with 95% CI) were obtained for each department. We indicate the 99th percentile (extreme heat) with red dotted lines, and with blue ones, we illustrate the 2.5th percentile (moderate cold).

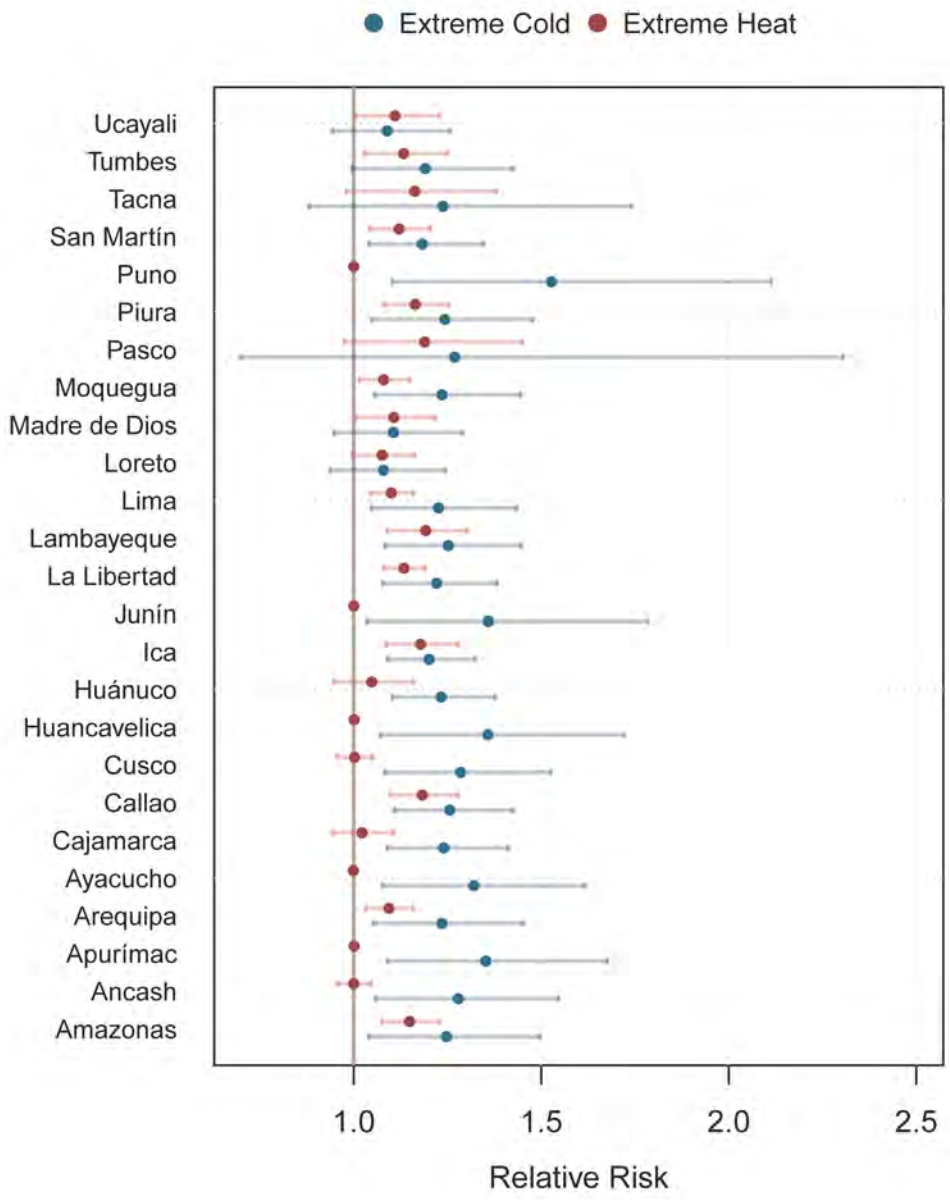

Figure S.5: Extreme heat and cold-related mortality relative risks (RR with 95% CI) for all Peru's departments between 2009 and 2019. The associations were estimated as the best linear unbiased predictions (BLUPs). Extreme cold was defined at the 1st percentile and extreme heat at the 99th percentile of the temperature distribution.

2.11 Supplementary Tables

Table S.1: Temperature and mortality data summarized by department.

Department	Provinces (n)	Total deaths	Temperature (°C)	
			Range	Mean
Amazonas	7	7,568	6.9	20.0
Ancash	20	39,335	3.0	14.3
Apurímac	7	13,391	2.8	11.9
Arequipa	8	58,159	6.9	14.3
Ayacucho	11	18,110	3.0	12.7
Cajamarca	13	34,120	3.1	16.8
Callao	1	53,274	5.0	19.9
Cusco	13	48,416	4.7	12.0
Huancavelica	7	15,099	3.1	11.5
Huánuco	11	27,477	4.2	15.6
Ica	5	38,424	4.7	20.6
Junín	9	54,205	3.4	11.7
La Libertad	12	79,319	6.1	18.0
Lambayeque	3	62,599	4.6	21.8
Lima	10	386,194	6.8	14.9
Loreto	8	14,352	1.3	26.8
Madre de Dios	3	5,375	1.5	26.7
Moquegua	3	6,358	6.5	13.9
Pasco	3	7,116	12.7	14.3
Piura	8	72,317	5.5	23.1
Puno	13	60,441	3.5	8.6
San Martín	10	19,704	3.6	23.6
Tacna	4	13,266	9.7	12.2
Tumbes	3	6,400	2.4	25.4
Ucayali	4	15,582	1.4	26.5
Total	**196**	**1,156,601**		

Table S.2: Summary of the mortality data categorized by sex and age.

Description	Total deaths	Percentage (%)
All-cause mortality	1,156,601	
Female	537,976	46.51
Male	618,625	53.49
All-cause mortality below 65 years	459,977	39.77
All-cause mortality 65 years and older	696,624	60.23

Table S.3: Mortality counts classified in 22 groups based on the ICD-10.

ICD Code	Description	Total deaths
A00 to B99	Certain infectious and parasitic diseases	92,088
C00 to D48	Neoplasms	221,129
D50 to D89	Diseases of the blood and blood-forming organs and certain disorders involving the immune mechanism	6,913
E00 to E90	Endocrine, nutritional and metabolic diseases	56,165
F00 to F99	Mental and behavioural disorders	1,612
G00 to G99	Diseases of the nervous system	22,810
H00 to H59	Diseases of the eye and adnexa	38
H60 to H95	Diseases of the ear and mastoid process	34
I00 to I99	Diseases of the circulatory system	201,243
J00 to J99	Diseases of the respiratory system	248,974
K00 to K93	Diseases of the digestive system	81,934
L00 to L99	Diseases of the skin and subcutaneous tissue	3,824
M00 to M99	Diseases of the musculoskeletal system and connective tissue	4,835
N00 to N99	Diseases of the genitourinary system	49,636
O00 to O99	Pregnancy, childbirth and the puerperium	1,749
P00 to P96	Certain conditions originating in the perinatal period	24,390
Q00 to Q99	Congenital malformations, deformations and chromosomal abnormalities	13,605
R00 to R99	Symptoms, signs and abnormal clinical and laboratory findings, not elsewhere classified	17,706
S00 to T98	Injury, poisoning and certain other consequences of external causes	489
U00 to U85	Codes for special purposes	11
V01 to Y98	External causes of morbidity and mortality	107,414
Z00 to Z99	Factors influencing health status and contact with health services	2
	Total	**1,156,601**

Table S.4: Aggregated mortality counts of the main six causes of death in Peru. The aggregation of the total counts was done based on the International Classification of Diseases, version 2019 (ICD-10).

ICD Code	Description	Total deaths	Percentage (%)
J00 to J99	Diseases of the respiratory system	248,974	21.53
C00 to D48	Neoplasms	221,129	19.12
I00 to I99	Diseases of the circulatory system	201,243	17.40
V01 to Y98	External causes of morbidity and mortality	107,414	9.29
A00 to B99	Certain infectious and parasitic diseases	92,088	7.96
K00 to K93	Diseases of the digestive system	81,934	7.08
	Total	**952,782**	**82.38**

Table S.5: Pooled estimates of MMT, extreme heat and cold-related Relative Risks (with 95% CI).

		Relative Risk (CI 95%)	
	MMT (°C)	Extreme Cold 1st percentile	Extreme Heat 99th percentile
All-cause mortality	21.98	1.219 [1.117 - 1.331]	1.086 [1.019 - 1.158]
Infectious and parasitic diseases (A00-B99)	15.09	1.029 [0.793 - 1.334]	0.985 [0.651 - 1.489]
Diseases of the respiratory system (J00-J99)	21.49	1.292 [0.967 - 1.725]	1.297 [1.031 - 1.631]
Neoplasms (C00-D48)	16.18	1.15 [0.957 - 1.383]	1.047 [0.868 - 1.264]
Diseases of the circulatory system (I00-I99)	22.14	1.558 [1.265 - 1.92]	1.035 [0.889 - 1.205]
External causes of mortality (V01-Y98)	19.20	1.124 [0.818 - 1.545]	0.997 [0.795 - 1.249]
Diseases of the digestive system (K00-K93)	22.14	1.463 [1.061 - 2.018]	0.969 [0.767 - 1.224]
All-cause mortality Female	21.81	1.204 [1.061 - 1.367]	1.058 [0.961 - 1.164]
All-cause mortality Male	21.98	1.222 [1.086 - 1.374]	1.108 [1.018 - 1.207]
All-cause mortality below 65 years	20.29	1.039 [0.899 - 1.201]	1.033 [0.917 - 1.162]
All-cause mortality 65 years and older	21.98	1.319 [1.175 - 1.481]	1.131 [1.035 - 1.234]

Table S.6: Minimum Mortality Temperature (MMT) and Minimum Mortality Temperature Percentile (MMP) values calculated for all-cause mortality, 65 years old and older individuals and population below 65 years old. MMT and MMP were calculated across all the departments of Peru.

Department	All-cause mortality		All-cause mortality, 65 years and older individuals		All-cause mortality, population below 65 years old	
	Minimum Mortality Temperature (°C)	Minimum Mortality Temperature Percentile (%)	Minimum Mortality Temperature (°C)	Minimum Mortality Temperature Percentile (%)	Minimum Mortality Temperature (°C)	Minimum Mortality Temperature Percentile (%)
Amazonas	25.0	85	24.9	84	25.2	87
Ancash	23.6	98	24.6	99	17.7	85
Apurímac	15.9	99	15.9	99	13.0	71
Arequipa	20.3	90	20.3	90	18.0	76
Ayacucho	17.0	99	17.0	99	14.2	75
Cajamarca	20.4	92	20.5	93	18.6	76
Callao	23.6	88	23.6	88	22.6	77
Cusco	21.3	96	21.6	97	15.0	82
Huancavelica	15.1	99	15.1	99	12.8	69
Huánuco	22.9	90	22.9	90	19.8	82
Ica	24.2	87	24.1	86	25.4	96
Junín	23.2	99	23.2	99	21.1	89
La Libertad	23.1	87	23.1	87	24.3	93
Lambayeque	25.2	84	25.2	84	27.1	98
Lima	21.5	89	21.5	89	22.3	91
Loreto	28.1	90	28.1	89	29.2	99
Madre de Dios	28.0	88	28.1	89	27.0	55
Moquegua	20.6	89	20.9	90	18.1	80
Pasco	23.0	85	22.9	83	9.7	25
Piura	26.8	85	26.7	84	27.5	91
Puno	21.5	99	21.5	99	12.3	86
San Martín	26.2	87	26.2	87	27.1	96
Tacna	19.0	88	19.0	88	17.3	76
Tumbes	27.1	87	27.1	87	26.0	61
Ucayali	27.7	88	27.8	89	26.7	56

Table S.7: Moderate and extreme heat and cold-related Relative Risks (RR). Extreme temperatures correspond to the 1st and 99th percentiles. Moderate temperatures are defined by the 2.5th and 97.5th percentiles.

Department	Relative Risk (CI 95%)			
	Extreme Cold	Moderate Cold	Moderate Heat	Extreme Heat
	1st percentile	2.5th percentile	97.5th percentile	99th percentile
Amazonas	1.247 [1.04 - 1.495]	1.215 [1.037 - 1.423]	1.091 [1.044 - 1.139]	1.149 [1.075 - 1.228]
Ancash	1.279 [1.058 - 1.546]	1.274 [1.063 - 1.526]	1 [0.983 - 1.018]	1 [0.957 - 1.046]
Apurímac	1.352 [1.09 - 1.676]	1.353 [1.105 - 1.657]	1.021 [0.959 - 1.087]	1.001 [0.997 - 1.005]
Arequipa	1.235 [1.051 - 1.451]	1.225 [1.068 - 1.405]	1.055 [1.016 - 1.095]	1.094 [1.032 - 1.159]
Ayacucho	1.32 [1.077 - 1.617]	1.32 [1.092 - 1.596]	1.011 [0.963 - 1.062]	0.999 [0.996 - 1.003]
Cajamarca	1.24 [1.089 - 1.411]	1.223 [1.092 - 1.37]	1.011 [0.962 - 1.061]	1.022 [0.944 - 1.106]
Callao	1.256 [1.109 - 1.423]	1.227 [1.104 - 1.364]	1.127 [1.066 - 1.191]	1.183 [1.096 - 1.277]
Cusco	1.285 [1.083 - 1.525]	1.287 [1.104 - 1.502]	1 [0.981 - 1.02]	1.002 [0.955 - 1.05]
Huancavelica	1.358 [1.072 - 1.721]	1.364 [1.097 - 1.697]	1.017 [0.957 - 1.08]	1.001 [0.996 - 1.007]
Huánuco	1.233 [1.103 - 1.377]	1.222 [1.107 - 1.349]	1.037 [0.953 - 1.128]	1.048 [0.947 - 1.159]
Ica	1.201 [1.091 - 1.323]	1.175 [1.082 - 1.276]	1.098 [1.046 - 1.152]	1.178 [1.087 - 1.277]
Junín	1.359 [1.036 - 1.783]	1.368 [1.053 - 1.777]	1.003 [0.979 - 1.028]	1 [0.998 - 1.002]
La Libertad	1.221 [1.078 - 1.382]	1.202 [1.076 - 1.343]	1.079 [1.046 - 1.114]	1.134 [1.081 - 1.189]
Lambayeque	1.252 [1.084 - 1.446]	1.216 [1.078 - 1.373]	1.111 [1.05 - 1.176]	1.192 [1.089 - 1.303]
Lima	1.226 [1.047 - 1.434]	1.21 [1.062 - 1.379]	1.061 [1.025 - 1.099]	1.1 [1.045 - 1.159]
Loreto	1.079 [0.937 - 1.244]	1.046 [0.928 - 1.178]	1.038 [0.989 - 1.09]	1.076 [0.997 - 1.161]
Madre de Dios	1.106 [0.948 - 1.29]	1.065 [0.935 - 1.212]	1.055 [0.995 - 1.12]	1.107 [1.007 - 1.218]
Moquegua	1.235 [1.056 - 1.445]	1.228 [1.073 - 1.405]	1.051 [1.006 - 1.098]	1.08 [1.016 - 1.149]
Pasco	1.269 [0.699 - 2.304]	1.259 [0.725 - 2.186]	1.098 [0.982 - 1.229]	1.189 [0.976 - 1.449]
Piura	1.243 [1.048 - 1.476]	1.21 [1.041 - 1.407]	1.095 [1.044 - 1.148]	1.164 [1.08 - 1.254]
Puno	1.527 [1.103 - 2.113]	1.542 [1.123 - 2.119]	1.013 [0.979 - 1.049]	1 [0.999 - 1.001]
San Martín	1.183 [1.041 - 1.345]	1.15 [1.033 - 1.28]	1.067 [1.021 - 1.115]	1.121 [1.043 - 1.204]
Tacna	1.238 [0.881 - 1.74]	1.235 [0.914 - 1.668]	1.095 [0.981 - 1.222]	1.163 [0.98 - 1.38]
Tumbes	1.191 [0.996 - 1.425]	1.155 [0.992 - 1.345]	1.072 [1.012 - 1.136]	1.133 [1.028 - 1.25]
Ucayali	1.089 [0.944 - 1.256]	1.058 [0.934 - 1.198]	1.058 [0.993 - 1.126]	1.11 [1.003 - 1.228]

Table S.8: Estimated number of deaths attributable to non-optimal temperatures (AN) used to calculate the attributable mortality fraction (AF) for the period 2009 to 2019 by department. The attributable number was obtained as an overall and for the heat and cold components. The 95% CIs are displayed in square brackets.

	Attributable Number		
Department	**Total**	**Cold**	**Heat**
Amazonas	623 [170 : 999]	608 [158 : 985]	15 [7 : 24]
Ancash	4042 [-1009 : 7993]	4042 [-1020 : 8009]	0 [-15 : 16]
Apurímac	1897 [-40 : 3480]	1899 [-38 : 3486]	-1 [-7 : 4]
Arequipa	7880 [4505 : 10939]	7825 [4423 : 10867]	55 [19 : 92]
Ayacucho	2523 [154 : 4509]	2524 [154 : 4521]	-1 [-8 : 6]
Cajamarca	3324 [1115 : 5223]	3305 [1087 : 5214]	19 [-65 : 95]
Callao	4296 [2674 : 5968]	3923 [2320 : 5582]	372 [207 : 543]
Cusco	6963 [2117 : 11089]	6960 [2087 : 11145]	3 [-89 : 96]
Huancavelica	2597 [277 : 4518]	2599 [278 : 4527]	-2 [-9 : 5]
Huánuco	2682 [1125 : 4034]	2669 [1108 : 4037]	13 [-20 : 44]
Ica	2723 [1546 : 3899]	2372 [1269 : 3531]	352 [181 : 527]
Junín	10856 [590 : 18735]	10857 [586 : 18740]	-1 [-7 : 6]
La Libertad	4114 [2369 : 5694]	3740 [1998 : 5358]	374 [209 : 530]
Lambayeque	2830 [1142 : 4555]	2165 [573 : 3800]	665 [308 : 1038]
Lima	19169 [11743 : 25820]	14998 [8226 : 21262]	4171 [1789 : 6518]
Loreto	333 [-535 : 1176]	306 [-579 : 1164]	27 [-7 : 62]
Madre de Dios	139 [-145 : 388]	109 [-173 : 371]	30 [-4 : 62]
Moquegua	659 [412 : 902]	635 [384 : 876]	24 [3 : 46]
Pasco	1017 [-1206 : 2390]	978 [-1226 : 2354]	39 [-7 : 83]
Piura	3159 [796 : 5624]	2516 [104 : 4937]	643 [283 : 993]
Puno	17019 [2671 : 27808]	17022 [2666 : 27818]	-3 [-10 : 5]
San Martín	847 [197 : 1476]	666 [66 : 1283]	181 [63 : 304]
Tacna	1020 [324 : 1640]	1003 [304 : 1619]	17 [-9 : 44]
Tumbes	232 [-82 : 549]	208 [-111 : 522]	23 [3 : 43]
Ucayali	387 [-560 : 1255]	344 [-613 : 1218]	43 [-7 : 92]

Table S.9: Estimated number of deaths attributable to non-optimal temperatures (AN) for the population below 65 years old. AN was used to calculate the attributable mortality fraction (AF) for the period 2009 to 2019 by department. The 95% CIs are displayed in square brackets.

	Attributable Number (All-cause mortality, population below 65 years old)		
Department	**Total**	**Cold**	**Heat**
Amazonas	113 [-313 : 454]	112 [-318 : 455]	1 [-9 : 11]
Ancash	768 [-504 : 1875]	735 [-228 : 1636]	33 [-609 : 624]
Apurímac	276 [12 : 521]	217 [-11 : 417]	59 [-153 : 256]
Arequipa	2006 [-526 : 4114]	1966 [-484 : 4025]	40 [-48 : 129]
Ayacucho	380 [-8 : 739]	351 [-94 : 721]	29 [-173 : 223]
Cajamarca	758 [9 : 1488]	718 [-26 : 1414]	40 [-228 : 303]
Callao	737 [-166 : 1589]	702 [-156 : 1499]	35 [-181 : 252]
Cusco	1378 [-28 : 2682]	1286 [-82 : 2451]	92 [-544 : 614]
Huancavelica	343 [-102 : 721]	317 [-206 : 745]	25 [-153 : 195]
Huánuco	876 [-133 : 1891]	854 [-152 : 1746]	23 [-144 : 184]
Ica	711 [-253 : 1691]	710 [-276 : 1710]	2 [-41 : 43]
Junín	2142 [-3102 : 5628]	2137 [-3180 : 5729]	4 [-183 : 175]
La Libertad	1142 [-719 : 2767]	1135 [-726 : 2792]	7 [-44 : 56]
Lambayeque	796 [-1951 : 2956]	796 [-1948 : 2987]	0 [-25 : 24]
Lima	4080 [-2046 : 9034]	3773 [-2465 : 9117]	307 [-1006 : 1527]
Loreto	438 [-978 : 1581]	438 [-979 : 1581]	0 [-2 : 2]
Madre de Dios	137 [-114 : 375]	72 [-58 : 189]	66 [-119 : 228]
Moquegua	189 [19 : 340]	166 [9 : 301]	23 [-17 : 62]
Pasco	228 [-429 : 555]	-159 [-456 : 53]	387 [-421 : 919]
Piura	617 [-1582 : 2626]	605 [-1629 : 2609]	13 [-155 : 177]
Puno	2413 [-842 : 5038]	2393 [-944 : 5027]	21 [-572 : 445]
San Martín	219 [-542 : 878]	218 [-573 : 889]	1 [-46 : 44]
Tacna	174 [-90 : 419]	144 [-139 : 411]	30 [-70 : 129]
Tumbes	136 [-50 : 311]	105 [-47 : 245]	31 [-45 : 101]
Ucayali	291 [-214 : 771]	170 [-135 : 465]	121 [-207 : 420]

Table S.10: Estimated number of deaths attributable to non-optimal temperatures (AN) for individuals 65 years and older. AN was used to calculate the attributable mortality fraction (AF) for the period 2009 to 2019 by department. The 95% CIs are displayed in square brackets.

Attributable Number (All-cause mortality, 65 years and older individuals)			
Department	**Total**	**Cold**	**Heat**
Amazonas	306 [-146 : 665]	298 [-154 : 658]	8 [3 : 13]
Ancash	3471 [-1544 : 7542]	3471 [-1547 : 7546]	0 [-4 : 4]
Apurímac	1775 [346 : 2888]	1776 [342 : 2890]	-1 [-6 : 3]
Arequipa	4891 [508 : 8529]	4856 [475 : 8462]	35 [-2 : 70]
Ayacucho	2185 [527 : 3536]	2186 [525 : 3538]	-1 [-6 : 4]
Cajamarca	2618 [671 : 4225]	2606 [656 : 4222]	12 [-36 : 58]
Callao	2915 [1112 : 4605]	2592 [853 : 4255]	323 [173 : 463]
Cusco	5240 [1857 : 7970]	5238 [1836 : 8034]	1 [-37 : 40]
Huancavelica	2095 [519 : 3312]	2096 [514 : 3318]	-1 [-7 : 5]
Huánuco	2266 [505 : 3739]	2257 [496 : 3713]	9 [-9 : 26]
Ica	2400 [1150 : 3638]	2032 [818 : 3241]	368 [214 : 517]
Junín	8631 [1581 : 13959]	8631 [1579 : 13961]	0 [-4 : 4]
La Libertad	3294 [1457 : 4909]	2900 [1128 : 4471]	393 [235 : 547]
Lambayeque	2674 [879 : 4461]	1980 [265 : 3652]	694 [395 : 979]
Lima	15682 [7556 : 22784]	11835 [4973 : 18074]	3847 [1330 : 6244]
Loreto	244 [-264 : 691]	227 [-294 : 672]	17 [-6 : 40]
Madre de Dios	57 [-66 : 165]	44 [-80 : 150]	14 [1 : 25]
Moquegua	520 [141 : 828]	501 [130 : 797]	18 [-6 : 42]
Pasco	1043 [-266 : 1728]	1018 [-284 : 1694]	25 [-5 : 50]
Piura	2822 [629 : 4942]	2144 [-67 : 4277]	677 [371 : 954]
Puno	12606 [3838 : 18695]	12608 [3838 : 18699]	-1 [-6 : 3]
San Martín	684 [184 : 1147]	530 [13 : 1001]	154 [74 : 224]
Tacna	506 [-116 : 1013]	497 [-120 : 1009]	8 [-12 : 27]
Tumbes	94 [-219 : 385]	76 [-239 : 358]	17 [3 : 31]
Ucayali	188 [-380 : 671]	164 [-402 : 655]	24 [-3 : 48]

Table S.11: Estimated attributable mortality fraction (AF) due to non-optimal temperatures from 2009 to 2019 by department for the population group below 65 years old. (All-cause mortality, population below 65 years old). The 95% CIs are displayed in square brackets.

Attributable Fraction (%) (All-cause mortality, population below 65 years old)			
Department	**Total**	**Cold**	**Heat**
Amazonas	3.25 [-8.95 : 13.00]	3.21 [-9.12 : 13.03]	0.04 [-0.25 : 0.31]
Ancash	5.43 [-3.57 : 13.27]	5.20 [-1.61 : 11.58]	0.23 [-4.31 : 4.42]
Apurímac	5.34 [0.23 : 10.08]	4.20 [-0.20 : 8.06]	1.14 [-2.97 : 4.95]
Arequipa	8.72 [-2.29 : 17.88]	8.54 [-2.10 : 17.49]	0.18 [-0.21 : 0.56]
Ayacucho	5.03 [-0.10 : 9.79]	4.64 [-1.24 : 9.55]	0.39 [-2.29 : 2.95]
Cajamarca	5.67 [0.07 : 11.14]	5.37 [-0.19 : 10.58]	0.30 [-1.71 : 2.27]
Callao	3.85 [-0.87 : 8.30]	3.67 [-0.82 : 7.83]	0.18 [-0.94 : 1.32]
Cusco	6.10 [-0.13 : 11.87]	5.69 [-0.36 : 10.85]	0.41 [-2.41 : 2.72]
Huancavelica	5.19 [-1.55 : 10.91]	4.81 [-3.12 : 11.29]	0.38 [-2.32 : 2.95]
Huánuco	7.16 [-1.08 : 15.45]	6.97 [-1.24 : 14.26]	0.19 [-1.18 : 1.50]
Ica	5.09 [-1.81 : 12.10]	5.08 [-1.98 : 12.24]	0.01 [-0.29 : 0.31]
Junín	9.18 [-13.30 : 24.13]	9.16 [-13.64 : 24.56]	0.02 [-0.78 : 0.75]
La Libertad	3.73 [-2.35 : 9.04]	3.71 [-2.37 : 9.12]	0.02 [-0.14 : 0.18]
Lambayeque	3.31 [-8.12 : 12.30]	3.31 [-8.11 : 12.43]	0.00 [-0.10 : 0.10]
Lima	2.94 [-1.48 : 6.52]	2.72 [-1.78 : 6.58]	0.22 [-0.73 : 1.10]
Loreto	5.38 [-12.01 : 19.42]	5.38 [-12.03 : 19.42]	0.00 [-0.03 : 0.02]
Madre de Dios	3.62 [-3.00 : 9.89]	1.89 [-1.53 : 4.97]	1.73 [-3.12 : 6.01]
Moquegua	8.53 [0.88 : 15.40]	7.51 [0.43 : 13.64]	1.03 [-0.78 : 2.81]
Pasco	6.37 [-12.01 : 15.53]	-4.45 [-12.76 : 1.49]	10.82 [-11.78 : 25.72]
Piura	2.18 [-5.59 : 9.28]	2.14 [-5.76 : 9.22]	0.04 [-0.55 : 0.63]
Puno	8.65 [-3.02 : 18.06]	8.58 [-3.38 : 18.03]	0.07 [-2.05 : 1.60]
San Martín	2.23 [-5.52 : 8.93]	2.22 [-5.83 : 9.04]	0.01 [-0.47 : 0.45]
Tacna	2.94 [-1.52 : 7.11]	2.43 [-2.36 : 6.96]	0.51 [-1.19 : 2.18]
Tumbes	4.71 [-1.72 : 10.80]	3.63 [-1.63 : 8.49]	1.08 [-1.58 : 3.52]
Ucayali	3.14 [-2.30 : 8.30]	1.83 [-1.45 : 5.00]	1.30 [-2.22 : 4.53]

Table S.12: Estimated attributable mortality fraction (AF) due to non-optimal temperatures between 2009 to 2019 by department for individuals aged 65 and older. (All-cause mortality, individuals aged 65 and older). The 95% CIs are displayed in square brackets.

Attributable Fraction (%) (All-cause mortality, 65 years and older individuals)			
Department	**Total**	**Cold**	**Heat**
Amazonas	7.51 [-3.59 : 16.33]	7.32 [-3.78 : 16.16]	0.20 [0.07 : 0.32]
Ancash	13.78 [-6.13 : 29.94]	13.78 [-6.14 : 29.95]	0.00 [-0.02 : 0.02]
Apurímac	21.61 [4.21 : 35.17]	21.63 [4.16 : 35.20]	-0.01 [-0.07 : 0.04]
Arequipa	13.97 [1.45 : 24.36]	13.87 [1.36 : 24.17]	0.10 [-0.01 : 0.20]
Ayacucho	20.71 [4.99 : 33.50]	20.71 [4.97 : 33.52]	-0.01 [-0.05 : 0.04]
Cajamarca	12.62 [3.23 : 20.36]	12.56 [3.16 : 20.34]	0.06 [-0.17 : 0.28]
Callao	8.60 [3.28 : 13.59]	7.65 [2.52 : 12.56]	0.95 [0.51 : 1.37]
Cusco	20.30 [7.20 : 30.87]	20.29 [7.11 : 31.12]	0.01 [-0.14 : 0.16]
Huancavelica	24.72 [6.12 : 39.06]	24.72 [6.06 : 39.14]	-0.01 [-0.08 : 0.06]
Huánuco	14.88 [3.32 : 24.55]	14.82 [3.25 : 24.38]	0.06 [-0.06 : 0.17]
Ica	9.83 [4.71 : 14.90]	8.32 [3.35 : 13.27]	1.51 [0.88 : 2.12]
Junín	27.96 [5.12 : 45.23]	27.97 [5.12 : 45.23]	0.00 [-0.01 : 0.01]
La Libertad	6.77 [2.99 : 10.09]	5.96 [2.32 : 9.19]	0.81 [0.48 : 1.12]
Lambayeque	6.96 [2.29 : 11.61]	5.15 [0.69 : 9.50]	1.81 [1.03 : 2.55]
Lima	6.33 [3.05 : 9.20]	4.78 [2.01 : 7.30]	1.55 [0.54 : 2.52]
Loreto	3.93 [-4.26 : 11.15]	3.66 [-4.74 : 10.84]	0.27 [-0.09 : 0.64]
Madre de Dios	3.70 [-4.27 : 10.59]	2.81 [-5.15 : 9.68]	0.90 [0.07 : 1.63]
Moquegua	12.56 [3.41 : 20.02]	12.12 [3.13 : 19.27]	0.44 [-0.15 : 1.02]
Pasco	29.62 [-7.56 : 49.06]	28.92 [-8.05 : 48.10]	0.70 [-0.14 : 1.43]
Piura	6.41 [1.43 : 11.23]	4.87 [-0.15 : 9.72]	1.54 [0.84 : 2.17]
Puno	38.77 [11.81 : 57.50]	38.77 [11.80 : 57.51]	0.00 [-0.02 : 0.01]
San Martín	6.93 [1.86 : 11.63]	5.37 [0.13 : 10.15]	1.56 [0.75 : 2.28]
Tacna	6.87 [-1.58 : 13.76]	6.76 [-1.64 : 13.71]	0.11 [-0.16 : 0.36]
Tumbes	2.66 [-6.22 : 10.97]	2.17 [-6.81 : 10.20]	0.50 [0.07 : 0.88]
Ucayali	2.99 [-6.04 : 10.66]	2.61 [-6.39 : 10.40]	0.38 [-0.04 : 0.77]

Chapter 3

Projected health impacts in the long-term future

This chapter describes and presents the estimated temperature-related mortality fractions that we obtained for the period 2071 to 2099. First, in subsection 3.1 we present the log-linear extrapolation of the exposure-response curves for the departments of Ica, Madre de Dios and Ucayali. The curves were generated using the information obtained in the second stage of the time series analysis. These information is described in Chapter 2, while the methodology can be consulted in Chapter 1. In summary, we used the BLUPs estimates and the values of MMT to extend the boundaries of the curves, specifically, the range of temperatures. Then, we used the `crosspred( )` function in R to illustrate the overall temperature-mortality association. In subsection 3.2, we present the projected excess mortality fractions due to non-optimal temperatures. The quantification of the projected mortality fractions is reported for both components, heat and cold under two climate scenarios, RCP 2.6 (mitigation scenario) and RCP 8.5 (high emissions scenario). The projected fractions were obtained under two main assumptions: a continuous population and the absence of adaptation measures.

3.1 Extrapolated temperature-mortality curves

Figure 1 illustrates the log-linear extrapolation of the temperature-mortality association for the department of Ica with 95% CI. The curve displays a typical J shape and shows the relative risk for two study periods: the observed period from 2009

to 2019 and the projected future, from 2071 to 2099. As we performed a log-linear extrapolation, the shape and estimates of the curve for the observed period did not change. This figure can be compared with the exposure-response curves that were obtained in the second stage (Figure S.3). However, what we can observe is that the range of temperatures shown on the X-axis increased, therefore, the RR raised as well.

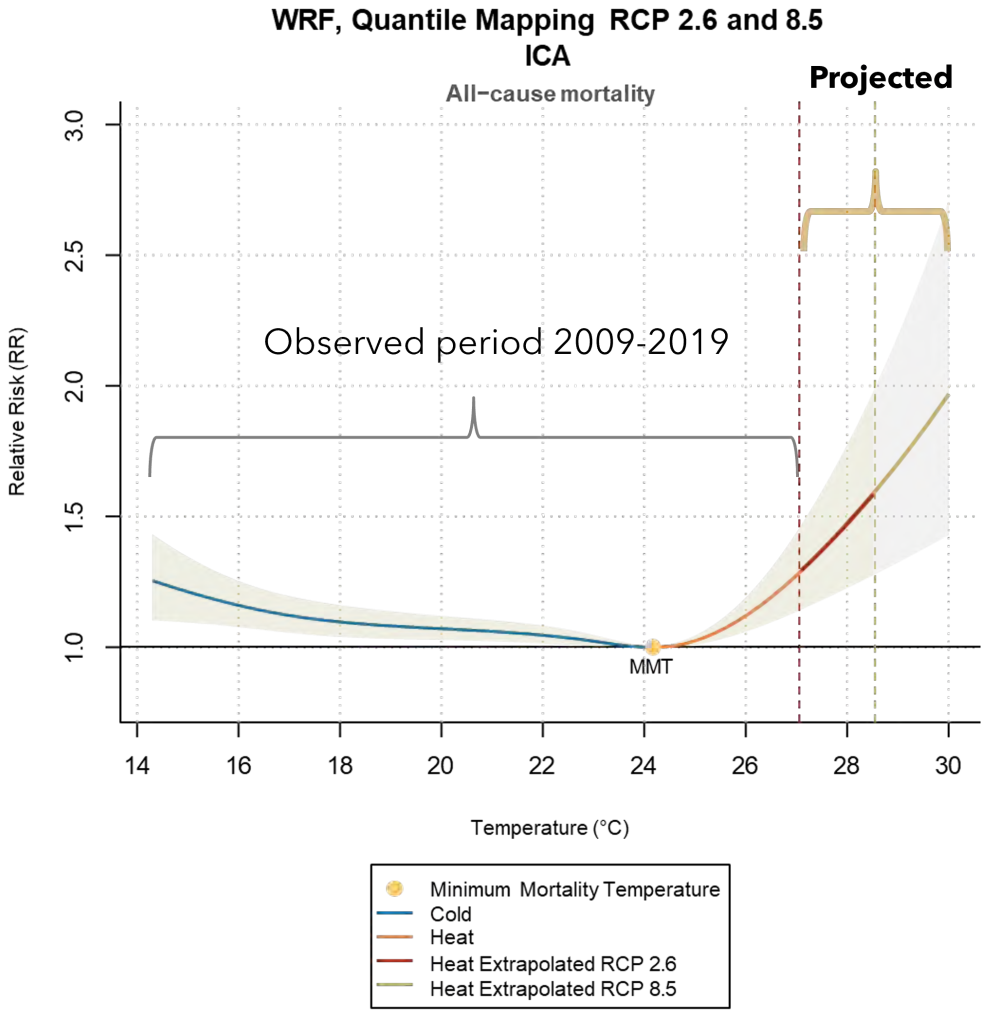

Figure 1: Extrapolation of the temperature-mortality association for the department of Ica with 95% CI. The CIs are shown in light green and transparent grey polygons, while different colour lines represent the RR estimates. In red colour, we highlight the RR estimates under a mitigation scenario (RCP 2.6), and the yellow dashed line indicates the RR under a high emissions scenario (RCP 8.5). The dashed red line indicates the maximum value of mean temperature under the scenario RCP 2.6, while the yellow one represents the minimum value of mean temperature under a high emissions scenario (RCP 8.5).

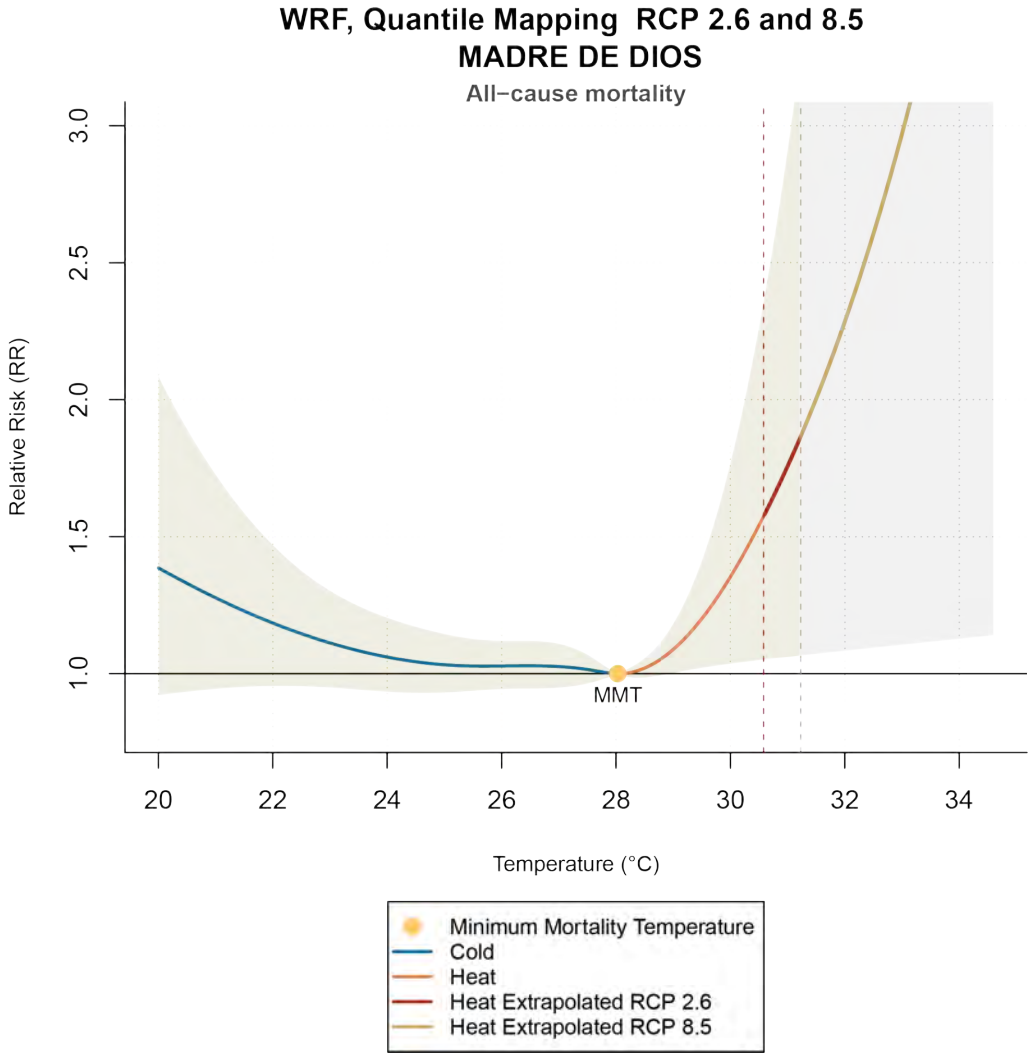

Figure 2: Extrapolation of the temperature-mortality association for the department of Madre de Dios with 95% CI. The CIs of the estimates are shown in light green and transparent grey polygons. The RR estimates are represented by different colour lines. The dashed red line indicates the maximum value of mean temperature under RCP 2.6 scenario, while the yellow one represents the minimum value of mean temperature under a high emissions scenario (RCP 8.5).

Figure 2 shows the extrapolation of the curve for the department of Madre de Dios. The relative risk (RR) obtained for this department increases the most under a high emissions scenario (RCP 8.5), with a projected temperature range increasing by approximately 3°C. However, the CIs of our estimates are not very robust. We hypothesise that the high variability in the CIs could be caused by the biases of the model that was used to simulate the future temperature values that we included in our analysis. Also, Madre de Dios is an area with few meteorological stations, therefore, the lack of observed temperature values that are available for this region

might increase the uncertainties and biases of our results. Nonetheless, the estimated RR under RCP 2.6 is more robust. Although the information of our extrapolation is not completely robust, it provides an overview of the future outcomes. In the Appendix, Figure A.1 illustrates the log-linear extrapolation of the curve for the department of Ucayali. The range of temperatures and shape of the curve are similar to those observed for Madre de Dios, even though both departments are not near each other. These similarities might be attributed to similar topographic conditions, however, to obtain the best estimation, further research and more robust datasets are needed.

3.2 Estimated temperature-mortality fractions for the period 2071 to 2099

We estimated the projected temperature-related mortality following the methodology of Vicedo et al. [58]. As explained in Chapter 1, we calibrated the temperature series generated with information from WRF simulations before doing the analysis. For this, we used the calibration function by Hempel et al. [62]. The calibration aimed to realign and correct biases of the simulated temperature values, therefore, for this correction, we used observed values to realign the series. We chose five overlapping years (2005 to 2010) from the PISCOt v1.2 dataset to do the bias correction to the historical and projected temperature series. For the calibration process, we first compared the distributions of the observed and historical temperature series from 2005 to 2010 for each analysed department. In the Appendix, Figure A.2 illustrates the distributions of the observed (PISCOt v1.2) and historical (WRF-QM) temperature series for each department over the overlapping period of 5 years (2005 to 2010).

Afterwards, to initiate the calibration, we implemented the function of Hempel et al. [62] in R to realign the series. To corroborate the calibration, we compared the cumulative distribution of the observed, simulated and calibrated temperature series. This is illustrated in the Appendix in Figure A.3 and Figure A.4. The first figure compares the calibrated temperature series under RCP 2.6, while the second one shows the comparison of the calibrated series under RCP 8.5. Finally, before starting the analysis to quantify the future health impacts, we compared the distribution of the historical and projected temperature series that were previously calibrated (See Figures A.5 and A.6 of the Appendix). With the calibrated

temperature series, we estimated the projected mortality fractions attributable to non-optimal temperatures, the results are reported in Table 1 and the comparison of the projected changes is illustrated in Figure 3. This analysis was not conducted by different age groups. Therefore, the results presented include all deaths across the entire population of the studied departments. To obtain the overall, heat and cold-related mortality fractions, we first calculated the attributable numbers, which are presented in Table A.1.

Table 1: Estimated attributable fraction to non-optimal temperatures for the period 2071 to 2099. The estimation was done for the historical (1981-2010) and for the future period (2071-2099) under two scenarios. The excess mortality was calculated for the cold and heat component, as well as the total.

Projected Attributable Fraction (%)						
	Historical			Future		
	Total			Total		
	Ica	Madre de Dios	Ucayali	Ica	Madre de Dios	Ucayali
WRF-QM-2.6	6.56 [3.60 : 9.66]	2.94 [-3.60 : 9.04]	2.75 [-4.07 : 9.10]	7.51 [4.32 : 10.47]	3.32 [-0.78 : 7.04]	3.12 [-1.16 : 6.70]
WRF-QM-8.5				12.54 [7.38 : 16.86]	23.87 [4.79 : 37.34]	23.78 [3.30 : 37.92]
	Cold			Cold		
	Ica	Madre de Dios	Ucayali	Ica	Madre de Dios	Ucayali
WRF-QM-2.6	6.37 [3.42 : 9.49]	2.68 [-3.94 : 8.83]	2.53 [-4.27 : 8.89]	3.90 [1.66 : 6.18]	1.43 [-2.51 : 5.06]	1.31 [-2.52 : 4.83]
WRF-QM-8.5				2.26 [0.78 : 3.69]	0.13 [-0.27 : 0.51]	0.09 [-0.19 : 0.36]
	Heat			Heat		
	Ica	Madre de Dios	Ucayali	Ica	Madre de Dios	Ucayali
WRF-QM-2.6	0.19 [0.08 : 0.31]	0.26 [-0.02 : 0.53]	0.22 [-0.02 : 0.47]	3.60 [1.96 : 5.17]	1.89 [0.16 : 3.51]	1.81 [0.11 : 3.50]
WRF-QM-8.5				10.28 [6.06: 13.99]	23.73 [4.63: 36.92]	23.69 [3.33 : 37.71]

Table 1 displays the results of our analysis by department. The estimates were calculated for both historical and future periods, considering mitigation and high emission scenarios. Contrary to the observed period, the projected estimates indicate a higher increase in mortality fraction caused by warmer temperatures, and a decline in cold-related mortality fractions. Our results show that the heat-related mortality fraction could potentially triple under a high emissions scenario (RCP 8.5) compared to the estimates obtained under a mitigation scenario (RCP 2.6). For Ucayali, the projections indicate that the heat-related mortality fraction would increase from 0.22% (95% CI: -0.02% to 0.47%) to 1.81% (95% CI: 0.11% to 3.5%) under mitigation conditions, and for a high emissions scenario, the proportion is estimated to increase by 23.69% (95% CI:3.33% to 37.71%). In Madre de Dios the fraction is projected to rise from 0.26% (95% CI: -0.02% to 0.53%) to 1.89% (95% CI: 0.16% to 3.51%) under a mitigation scenario (RCP. 2.6) and to 23.73% (95% CI: 4.63% to 36.92%) under a high emissions scenario (RCP 8.5). Moreover, for the department of Ica, the

estimated heat-related mortality fraction is projected to increase from 0.19% (95% CI: 0.08% to 0.31%) to 3.60% (95% CI: 1.96% to 5.17%) under RCP 2.6 and 10.28% (95% CI: 6.06% to 13.99%) for RCP 8.5.

Figure 3 illustrates the projected changes in the future attributable mortality fractions obtained under RCP 2.6 and RCP 8.5 conditions. In all departments, future cold-related mortality is projected to decrease compared to the historical baseline estimates. Although this reduction is most noticeable for the estimates obtained under a high emissions scenario (RCP 8.5), the cold excess mortality fraction decrease does not compensate for the projected increase in excess mortality fraction related to heat. Nevertheless, it is important to emphasize that our results were obtained under 2 key assumptions: no changes in the population and no adaptation measures implemented in the future.

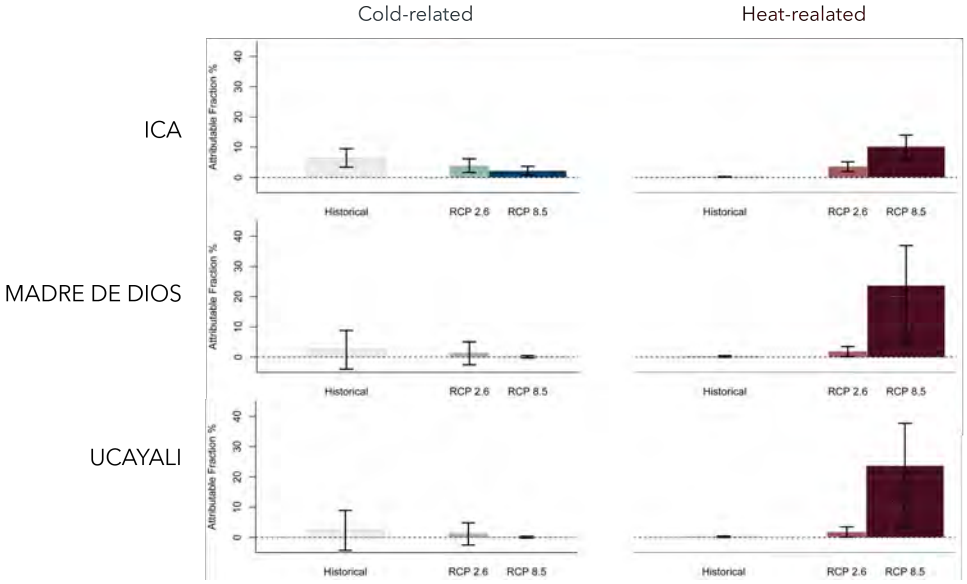

Figure 3: Projected attributable mortality fraction due to non-optimal warm and cold temperatures for the period 2071 to 2099. The estimation was done for the historical (1981-2010) and for the future period (2071-2099) under two scenarios. The estimated mortality fractions are shown for the cold and heat components.

Chapter 4

Conclusion and key findings

In this master's thesis project, we aimed to quantify the health impacts of non-optimal temperatures in Peru for present and future conditions. Our results showed that for the observed period, 8.77% of the total all-cause mortality was attributed to non-optimal heat and cold temperatures. We found that most of the attributable mortality fraction was linked to non-optimal cold temperatures, and our calculations showed that the majority of the cold-related mortality fraction occurred in the departments located in southern Peru. Due to the limitations on the spatial coverage of the future climate projections, we were not able to quantify the projected impacts of non-optimal temperatures for all departments of Peru. Thus, we only analysed the departments of Ica, Madre de Dios and Ucayali. Our findings indicate that for the projected period from 2071 to 2099, cold-related mortality is anticipated to decrease compared to the historical estimates. Nonetheless, heat-related mortality is expected to increase across all studied departments, surpassing the projected reduction in the mortality fraction attributable to non-optimal cold temperatures.

Although we did not find differences in the relative risk obtained for the stratified analysis between male and female populations for the observed period, we identified that individuals aged 65 years and older were the most vulnerable when exposed to non-optimal temperatures, mainly to cold ones. By pooling the estimates for different causes of death, we found that exposure to extreme cold significantly increased mortality risk among individuals with underlying circulatory system conditions. We also calculated the mortality risks for exposure to extreme heat and cold for all-age all-cause mortality. Our results showed that for the departments located in coastal areas in the north of Peru, the mortality risk was higher when populations were

exposed to extreme heat. However, exposure to extreme cold impacted the most in the south of the country, specifically in the department of Puno. In Peru, the departments of Puno, Junín, Huancavelica, Ayacucho, and Arequipa experience the most extreme cold [53]. Our stratified analysis showed that the department of Puno experienced the highest attributable mortality fraction due to non-optimal cold temperatures. We estimated that in Puno non-optimal cold was linked to 38.77% (95% CI: 11.80% to 57.51%) among the elderly population (aged 65 and older) and 8.58% (95% CI: -3.38% to 18.03%) among younger individuals.

By conducting an extended two-stage time series small-area analysis, we were able to obtain the temperature-mortality associations for all departments considering mortality counts from all Peruvian provinces. In addition, we quantified the attributable mortality fraction linked to non-optimal temperatures. However, temperature-related mortality is not just influenced by temperature and climatic conditions, but it is also determined by demographic and socioeconomic factors [97]. Thus, our findings provide nationwide information that should be considered by policymakers and stakeholders when designing and implementing mitigation and adaptation programs to reduce the vulnerability of populations exposed to non-optimal heat and cold temperatures. Special emphasis should be given to the department of Puno, which in 2021 was identified as one of the departments most vulnerable to poverty [52], and where our analysis revealed the highest attributable fraction linked to non-optimal temperatures.

We were not able to estimate the projected temperature-related mortality for all the departments of Peru. Nonetheless, our results illustrate that in some areas heat-related mortality could increase by 20% under a high emissions scenario. Hence, considerable preventative and adaptation measures must be implemented to protect the most vulnerable populations. In 2020, Aracena et al. [98] analyzed the policies and adaptation plans that aimed at addressing the impacts of climate change on Peru's health systems. The results of the analysis indicated that most of the Peruvian departments presented adaptation strategies to cope with the projected impacts of climate on health. However, vulnerable populations and marginalized groups were not addressed properly in their strategies, and the reduced research at a local level presented a challenge to develop strategic plans. Therefore, additional research including socioeconomic factors should be conducted to provide a concise local overview of the projected climate change impacts. Thus, the results presented in this master's thesis can serve as a foundation for further research in Peru.

5. References

[1] GBD 2019 Risk Factors Collaborators. Global burden of 87 risk factors in 204 countries and territories, 1990–2019: a systematic analysis for the Global Burden of Disease Study 2019. The Lancet. 2020;396(10258):1223-49.

[2] Zhao Q, Guo Y, Ye T, Gasparrini A, Tong S, Overcenco A, et al. Global, regional, and national burden of mortality associated with non-optimal ambient temperatures from 2000 to 2019: a three-stage modelling study. The Lancet Planetary Health. 2021;5(7):e415-25.

[3] IPCC. Climate Change 2023: Synthesis Report. Contribution of Working Groups I, II and III to the Sixth Assessment Report of the Intergovernmental Panel on Climate Change. [Core Writing Team and Hoesung Lee and José Romero (eds.)]. Geneva, Switzerland: IPCC; 2023.

[4] WMO (World Meteorological Organization). State of the Climate in Latin America and the Caribbean 2021. WMO; 2022.

[5] Economic Commission for Latin America and the Caribbean (ECLAC). Demographic Observatory. Latin America and the Caribbean 2023: Population dynamics in Latin America and their effects on the labour force. (LC/PUB.2023/26-P/Rev.1). Santiago, Chile: ECLAC; 2024.

[6] Cissé G, McLeman R, Adams H, Aldunce P, Bowen K, Campbell-Lendrum D, et al. Health, Wellbeing, and the Changing Structure of Communities. In: Pörtner HO, Roberts DC, Tignor MMB, Poloczanska ES, Mintenbeck K, Alegría A, et al., editors. Climate Change 2022: Impacts, Adaptation and Vulnerability. Contribution of Working Group II to the Sixth Assessment Report of the Intergovernmental Panel on Climate Change. Cambridge, UK and New York, USA: Cambridge University Press; 2022. p. 1041-170.

[7] GBD 2019 Diseases and Injuries Collaborators. Global burden of 369 diseases and injuries in 204 countries and territories, 1990–2019: a systematic analysis for the Global Burden of Disease Study 2019. The Lancet. 2020;396(10258):1204-22.

[8] Burkart KG, Brauer M, Aravkin AY, Godwin WW, Hay SI, He J, et al. Estimating the cause-specific relative risks of non-optimal temperature on daily mortality: a two-part modelling approach applied to the Global Burden of Disease Study. The Lancet. 2021;398(10301):685-97.

[9] Gasparrini A, Guo Y, Hashizume M, Lavigne E, Zanobetti A, Schwartz J, et al. Mortality risk attributable to high and low ambient temperature: a multicountry observational study. The Lancet. 2015;386(9991):369-75.

[10] de Schrijver E, Bundo M, Ragettli MS, Sera F, Gasparrini A, Franco OH, et al. Nationwide Analysis of the Heat- and Cold-Related Mortality Trends in Switzerland between 1969 and 2017: The Role of Population Aging. Environmental Health Perspectives. 2022;130(3).

[11] Masselot P, Mistry M, Vanoli J, Schneider R, Iungman T, Garcia-Leon D, et al. Excess mortality attributed to heat and cold: a health impact assessment study in 854 cities in Europe. The Lancet Planetary Health. 2023;7(4):e271-81.

[12] Petkova EP, Dimitrova LK, Sera F, Gasparrini A. Mortality attributable to heat and cold among the elderly in Sofia, Bulgaria. International Journal of Biometeorology. 2021;65(6):865-72.

[13] Kephart JL, Sánchez BN, Moore J, Schinasi LH, Bakhtsiyarava M, Ju Y, et al. City-level impact of extreme temperatures and mortality in Latin America. Nature Medicine. 2022;28(8):1700—1705.

[14] Gasparrini A, Masselot P, Scortichini M, Schneider R, Mistry MN, Sera F, et al. Small-area assessment of temperature-related mortality risks in England and Wales: a case time series analysis. The Lancet Planetary Health. 2022;6(7):e557-64.

[15] Cheng J, Xu Z, Bambrick H, Su H, Tong S, Hu W. Impacts of heat, cold, and temperature variability on mortality in Australia, 2000–2009. Science of The Total Environment. 2019;651:2558-65.

[16] Vicedo-Cabrera AM, Scovronick N, Sera F, Royé D, Schneider R, Tobias A, et al. The burden of heat-related mortality attributable to recent human-induced climate change. Nature Climate Change. 2021;11(6):492-500.

[17] Aboubakri O, Khanjani N, Jahani Y, Bakhtiari B, Mesgari E. Projection of mortality attributed to heat and cold; the impact of climate change in a dry region of Iran, Kerman. Science of The Total Environment. 2020;728(138700).

[18] de Schrijver E, Sivaraj S, Raible CC, Franco OH, Chen K, Vicedo-Cabrera AM. Nationwide projections of heat- and cold-related mortality impacts under various climate change and population development scenarios in Switzerland. Environmental Research Letters. 2023;18(094010).

[19] Achebak H, Devolder D, Ingole V, Ballester J. Reversal of the seasonality of temperature-attributable mortality from respiratory diseases in Spain. Nature Communications. 2020;11(2457).

[20] Martinez GS, Diaz J, Hooyberghs H, Lauwaet D, De Ridder K, Linares C, et al. Cold-related mortality vs heat-related mortality in a changing climate: A case study in Vilnius (Lithuania). Environmental Research. 2018;166:384-93.

[21] Huang J, Li G, Liu Y, Huang J, Xu G, Qian X, et al. Projections for temperature-related years of life lost from cardiovascular diseases in the elderly in a Chinese city with typical subtropical climate. Environmental Research. 2018;167:614-21.

[22] Vardoulakis S, Dear K, Hajat S, Heaviside C, Eggen B, McMichael AJ. Comparative Assessment of the Effects of Climate Change on Heat- and Cold-Related Mortality in the United Kingdom and Australia. Environmental Health Perspectives. 2014;122(12):1285-92.

[23] Tansey EA, Johnson CD. Recent advances in thermoregulation. Advances in Physiology Education. 2015;39(3):139-48.

[24] Margolis HG. Heat Waves and Rising Temperatures: Human Health Impacts and the Determinants of Vulnerability. In: Pinkerton KE, Rom WN, editors. Climate Change and Global Public Health. Springer International Publishing; 2021. p. 123-61.

[25] Hall JE. Body Temperature Regulation and Fever. In: Guyton and Hall Textbook of Medical Physiology. 13th ed. Philadelphia, PA: Elsevier; 2016. p. 910-22.

[26] Wenger CB. The regulation of body temperature. In: Rhoades RA, Tanner GA, editors. Medical Physiology. 2nd ed. Philadelphia, PA: Lippincott Williams & Wilkins; 2003. p. 527–550.

[27] Kuht J, Farmery AD. Body temperature and its regulation. Anaesthesia & Intensive Care Medicine. 2014;15(6):273-8.

[28] Maniar A, Koh KF. Heat balance and anaesthetic implications in the elderly. In: Dodds C, Kumar C, Veering B, editors. Oxford Textbook of Anaesthesia for the Elderly Patient. Oxford University Press; 2014. p. 280-7.

[29] Kathryn E Cooper. Basic Thermoregulation. In: Greger R, Windhorst U, editors. Comprehensive Human Physiology: From Cellular Mechanisms to Integration. vol. 1. Berlin, Heidelberg: Springer; 1996. p. 2199-206.

[30] Chambers D, Huang C, Matthews G. Temperature Regulation. In: Basic Physiology for Anaesthetists. Cambridge: Cambridge University Press; 2019. p. 436–438.

[31] Hughes SJ. Scientific principles. In: Hughes SJ, editor. Oxford Handbook of Perioperative Practice. Oxford University Press; 2022. p. 257-72.

[32] Seltenrich N. Between extremes: Health effects of heat and cold. Environmental Health Perspectives. 2015;123(11):275-9.

[33] Sessler DI. Thermoregulatory defense mechanisms. Critical Care Medicine. 2009;37(7).

[34] Sargent F. The mechanism of hidromeiosis. International Journal of Biometeorology. 1961;5:37-40.

[35] Candas V, Libert JP, Vogt JJ. Effect of hidromeiosis on sweat drippage during acclimation to humid heat. European Journal of Applied Physiology and Occupational Physiology. 1980;44:123-33.

[36] Wissler EH. Sweating. In: Human Temperature Control: A Quantitative Approach. Berlin, Heidelberg: Springer; 2018. p. 197-237.

[37] Banerjee A. Temperature Regulation. In: Clinical Physiology: An Examination Primer. Cambridge: Cambridge University Press; 2005. p. 66–70.

[38] Wissler EH. Conservation of Energy. In: Human Temperature Control: A Quantitative Approach. Berlin, Heidelberg: Springer; 2018. p. 17-40.

[39] Ahmadalipour A, Moradkhani H, Kumar M. Mortality risk from heat stress expected to hit poorest nations the hardest. Climatic Change. 2019;152:569-79.

[40] Banerjee A. Neurophysiology. In: Clinical Physiology: An Examination Primer. Cambridge: Cambridge University Press; 2005. p. 177–257.

[41] Perera F. Not Just Little Adults. In: Perera F, editor. Children's Health and the Peril of Climate Change. Oxford University Press; 2022. p. 24-45.

[42] United Nations Children's Fund. The Climate Crisis is a Child Rights Crisis: Introducing the Children's Climate Risk Index. New York: UNICEF; 2021.

[43] Forzieri G, Cescatti A, e Silva FB, Feyen L. Increasing risk over time of weather-related hazards to the European population: a data-driven prognostic study. The Lancet Planetary Health. 2017;1(5):e200-8.

[44] Wissler EH. Shivering. In: Human Temperature Control: A Quantitative Approach. Berlin, Heidelberg: Springer; 2018. p. 239-64.

[45] UNDP (United Nations Development Programme). Global Multidimensional Poverty Index 2023. Unstacking global poverty: Data for high impact action. New York: UNDP; 2023.

[46] UNDRR (United Nations Office for Disaster Risk Reduction) and OCHA (UN Office for the Coordination of Humanitarian Affairs). Overview of Disasters in Latin America and the Caribbean 2000 – 2022. UNDRR; 2023.

[47] Marchitto B, Conde J, Santos R, de Nicola C, Ferrazzi M, Baldini A, et al. Climate risks for Latin America and the Caribbean: Are banks ready for the green transition? European Investment Bank; 2023.

[48] WHO (World Health Organization). Quantitative risk assessment of the effects of climate change on selected causes of death, 2030s and 2050s. Switzerland: WHO; 2014.

[49] National Institute of Statistics and Informatics. A glimpse of Peru in figures. INEI; 2023.

[50] Bergmann J, Vinke K, Palomino CAF, Gornott C, Gleixner S, Laudien R, et al. Assessing the Evidence: Climate Change and Migration in Peru. Potsdam and Geneva: Potsdam Institute for Climate Impact Research (PIK) and International Organization for Migration (IOM); 2021.

[51] World Bank. Rising Strong: Peru Poverty and Equity Assessment. Washington, D.C: The World Bank; 2023.

[52] World Bank. Chapter 4: Vulnerability to Shocks and Climate Change. Washington, D.C: World Bank Group; 2023.

[53] National System for Disaster Risk Management (SINAGERD), Presidency of the Council of Ministers (PCM), Secretariat for Disaster Risk Management (SGRD), National Centre for Disaster Risk Estimation and Prevention and Reduction (CENEPRED), National Institute of Civil Defence (INDECI). Plan Nacional de Gestión del Riesgo de Desastres (National Plan for Disaster Risk Management) 2014–2021. Lima,Perú: Publimagen ABC; 2014.

[54] United Nations Children's Fund. The Coldest Year of the Rest of their Lives: Protecting children form the escalating impacts of heatwaves. New York: UNICEF; 2022.

[55] Andrews O, Quéré CL, Kjellstrom T, Lemke B, Haines A. Implications for workability and survivability in populations exposed to extreme heat under climate change: a modelling study. The Lancet Planetary Health. 2018;2(12):e540-7.

[56] Chen K, de Schrijver E, Sivaraj S, Sera F, Scovronick N, Jiang L, et al. Impact of population aging on future temperature-related mortality at different global warming levels. Nature Communications. 2024;15(1796).

[57] Bakhtsiyarava M, Schinasi LH, Sánchez BN, Dronova I, Kephart JL, Ju Y, et al. Modification of temperature-related human mortality by area-level socioeconomic and demographic characteristics in Latin American cities. Social Science & Medicine. 2023;317(115526).

[58] Vicedo-Cabrera AM, Sera F, Gasparrini A. Hands-on Tutorial on a Modeling Framework for Projections of Climate Change Impacts on Health. Epidemiology. 2019;30(3):321-9.

[59] Gasparrini A. A tutorial on the case time series design for small-area analysis. BMC Medical Research Methodology. 2022;22(129).

[60] Pedersen TL, Crameri F. scico: Colour Palettes Based on the Scientific Colour-Maps; 2024. R package version 1.5.0.9000. Available from: `https://github.com/thomasp85/scico`.

[61] Huerta A, Aybar C, Imfeld N, Correa K, Felipe-Obando O, Rau P, et al. High-resolution grids of daily air temperature for Peru - the new PISCOt v1.2 dataset. Scientific Data. 2023;10(847).

[62] Hempel S, Frieler K, Warszawski L, Schewe J, Piontek F. A trend-preserving bias correction - the ISI-MIP approach. Earth System Dynamics. 2013;4:219-36.

[63] Instituto Nacional de Estadística e Informática. Perú: Estimaciones y Proyecciones de Población por Departamento, Provincia y Distrito, 2018-2020. Lima: INEI; 2020.

[64] González-Rojí SJ, Messmer M, Raible CC, Stocker TF. Climate Analysis of Peru. 2023.

[65] Baston D. exactextractr: Fast Extraction from Raster Datasets using Polygons; 2023. R package version 0.10.0. Available from: `https://CRAN.R-project.org/package=exactextractr`.

[66] Skamarock WC, Klemp JB, Dudhia J, Gill DO, Barker D, Duda MG, et al. A Description of the Advanced Research WRF Version 3. (No. NCAR/TN-475+STR). University Corporation for Atmospheric Research; 2008.

[67] R Core Team and contributors worldwide. base: The R Base Package; 2024. R package version 4.5.0. Available from: `https://www.r-project.org`.

[68] Gasparrini A, Armstrong B, Scheipl F. dlnm: Distributed Lag Non-Linear Models; 2021. R package version 2.4.7. Available from: `https://github.com/gasparrini/dlnm`.

[69] Gasparrini A, Armstrong B, Kenward MG. Distributed lag non-linear models. Statistics in Medicine. 2010;29(21):2224-34.

[70] Sera F, Armstrong B, Blangiardo M, Gasparrini A. An extended mixed-effects framework for meta-analysis. Statistics in Medicine. 2019;38(29):5429-44.

[71] Gasparrini A, Sera F. mixmeta: An Extended Mixed-Effects Framework for Meta-Analysis; 2021. R package version 1.2.0. Available from: `https://github.com/gasparrini/mixmeta`.

[72] Sera F, Gasparrini A. Extended two-stage designs for environmental research. Environmental Health. 2022;21(41).

[73] Gasparrini A, Leone M. Attributable risk from distributed lag models. BMC Medical Research Methodology. 2014;14(55):1-8.

[74] Ripley B, Venables B, Bates DM, Hornik K, Gebhardt A, Firth D. MASS: Support Functions and Datasets for Venables and Ripley's MASS; 2023. R package version 7.3-61. Available from: `http://www.stats.ox.ac.uk/pub/MASS4/`.

[75] Ballester J, Quijal-Zamorano M, Turrubiates RFM, Pegenaute F, Herrmann FR, Robine JM, et al. Heat-related mortality in Europe during the summer of 2022. Nature Medicine 2023 29:7. 2023;29(7):1857-66.

[76] Seneviratne SI, Zhang X, Adnan M, Badi W, Dereczynski C, Luca AD, et al. Weather and Climate Extreme Events in a Changing Climate. In: Masson-Delmotte V, Zhai P, Pirani A, Connors SL, Péan C, Berger S, et al., editors. Climate Change 2021: The Physical Science Basis. Contribution of Working Group I to the Sixth Assessment Report of the Intergovernmental Panel on Climate Change. Cambridge, United Kingdom and New York, NY, USA: Cambridge University Press; 2021. p. 1513-766.

[77] Lüthi S, Fairless C, Fischer EM, Scovronick N, Armstrong B, Coelho MDSZS, et al. Rapid increase in the risk of heat-related mortality. Nature Communications. 2023;14(4894).

[78] Gasparrini A, Guo Y, Sera F, Vicedo-Cabrera AM, Huber V, Tong S, et al. Projections of temperature-related excess mortality under climate change scenarios. The Lancet Planetary Health. 2017;1(9):e360-7.

[79] Inter-American Development Bank, Ezquiaga Arquitectura, Sociedad y Territorio S L . The Experience of Latin America and the Caribbean in Urbanization. Knowledge Sharing Forum on Development Experiences: Comparative Experiences of Korea and Latin America and the Caribbean. Inter-American Development Bank (IDB); 2015.

[80] UN-HABITAT. Habitat III: Regional Report from Latin America and The Caribbean. United Nations Human Settlements Programme (UN-HABITAT); 2018.

[81] Rodgers D, Beall J, Kanbur R. Latin American Urban Development into the Twenty First Century: Towards a renewed perspective on the city. 4. Palgrave Macmillan London; 2012.

[82] R Core Team. R: A Language and Environment for Statistical Computing; 2023. R (version 4.3.2). Available from: `https://www.R-project.org/`.

[83] Ministry of Health of Peru (MINSA). Resolución Ministerial N° 280-2016-RM; 2016. Accessed: 28-11-2023. Available from: `https://www.gob.pe/es/l/862704`.

[84] Muñoz-Sabater J, Dutra E, Agustí-Panareda A, Albergel C, Arduini G, Balsamo G, et al. ERA5-Land: a state-of-the-art global reanalysis dataset for land applications. Earth System Science Data. 2021;13(9):4349–4383.

[85] World Health Organization. International Statistical Classification of Diseases and Related Health Problems. ICD-10 Version: 2019;. Accessed: 2023-11-30. `https://icd.who.int/browse10/2019/en`.

[86] Vicedo-Cabrera AM, de Schrijver E, Schumacher DL, Ragettli MS, Fischer EM, Seneviratne SI. The footprint of human-induced climate change on heat-related deaths in the summer of 2022 in Switzerland. Environmental Research Letters. 2023;18(7):074037.

[87] Chen K, Wolf K, Breitner S, Gasparrini A, Stafoggia M, Samoli E, et al. Two-way effect modifications of air pollution and air temperature on total natural and cardiovascular mortality in eight European urban areas. Environment International. 2018;116:186-96.

[88] Zafeiratou S, Samoli E, Analitis A, Dimakopoulou K, Giannakopoulos C, Varotsos KV, et al. Modification of heat-related effects on mortality by air pollution concentration, at small-area level, in the Attica prefecture, Greece. Environmental Health. 2024;23(10).

[89] Stafoggia M, Michelozzi P, Schneider A, Armstrong B, Scortichini M, Rai M, et al. Joint effect of heat and air pollution on mortality in 620 cities of 36 countries. Environment International. 2023;181(108258).

[90] Rai M, Stafoggia M, de'Donato F, Scortichini M, Zafeiratou S, Vazquez Fernandez L, et al. Heat-related cardiorespiratory mortality: Effect modification by air pollution across 482 cities from 24 countries. Environment International. 2023;174(107825).

[91] Steenland K, Vu B, Scovronick N. Effect modification by maximum temperature of the association between PM2.5 and short-term cardiorespiratory mortality and emergency room visits in Lima, Peru, 2010–2016. Journal of Exposure Science & Environmental Epidemiology. 2022;32(4):590-5.

[92] Tapia VL, Vasquez-Apestegui BV, Alcantara-Zapata D, Vu B, Steenland K, Gonzales GF. Association between maximum temperature and PM2.5 with pregnancy outcomes in Lima, Peru. Environmental Epidemiology. 2021;5(6).

[93] Deng P, Li Y, Li S, Feng Y, Jin D, Yang Y, et al. The role of high humidity on extreme-temperature-related mortality in central China. Air Quality, Atmosphere & Health. 2023;16(11):2285-95.

[94] Liang C, Yuan J, Tang X, Kan H, Cai W, Chen J. The influence of humid heat on morbidity of megacity Shanghai in China. Environment International. 2024;183(108424).

[95] Chen X, Zhu T, Wang Q, Wang T, Chen W, Yao Y, et al. Higher temperature and humidity exacerbate pollutant-associated lung dysfunction in the elderly. Environmental Research. 2024;245(118039).

[96] Feierherd G, Larroulet P, Long W, Lustig N. The Pink Tide and Income Inequality in Latin America. Latin American Politics and Society. 2023;65(2):110–144.

[97] Sera F, Armstrong B, Tobias A, Vicedo-Cabrera AM, Åström C, Bell ML, et al. How urban characteristics affect vulnerability to heat and cold: a multi-country analysis. International Journal of Epidemiology. 2019;48(4):1101-12.

[98] Aracena S, Barboza M, Zamora V, Salaverry O, Montag D. Health system adaptation to climate change: a Peruvian case study. Health Policy and Planning. 2021;36(1):45-83.

Appendix A

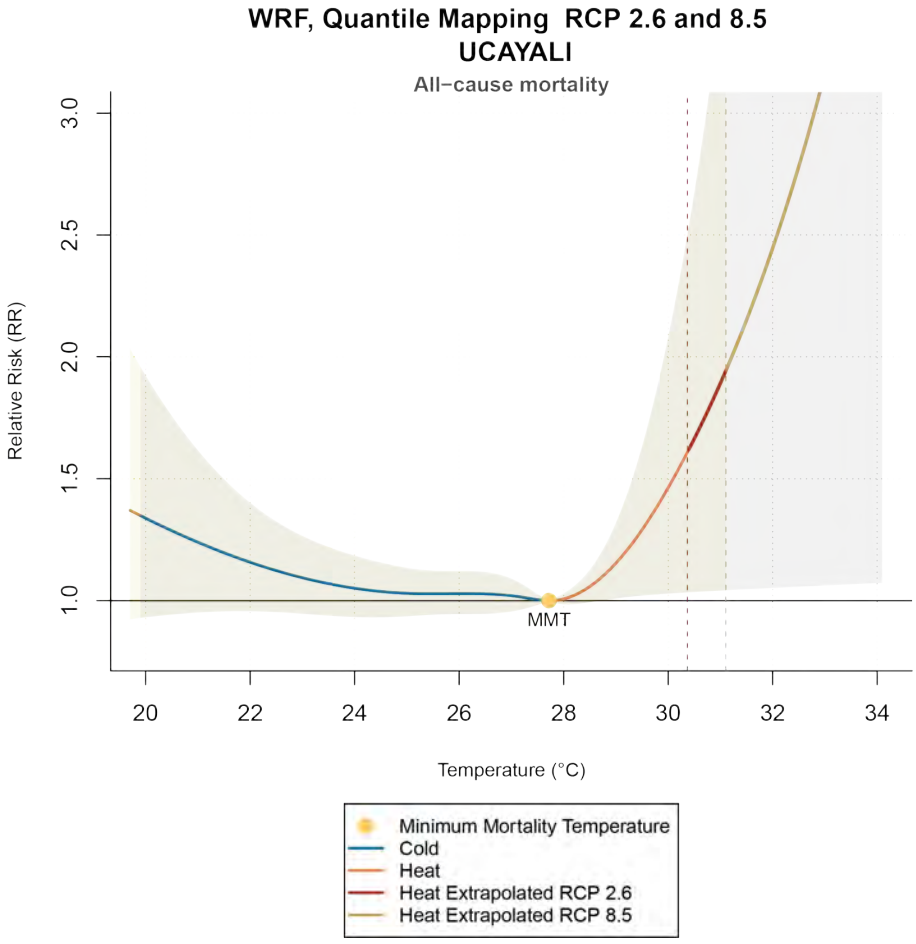

Figure A.1: Extrapolation of the temperature-mortality association for the department of Ucayali with 95% CI. The CIs are shown in light green and transparent grey polygons, while the RR estimates are represented by different colour lines. The dashed red line indicates the maximum value of mean temperature under the scenario RCP 2.6, while the yellow one represents the minimum value of mean temperature under a high emissions scenario (RCP 8.5).

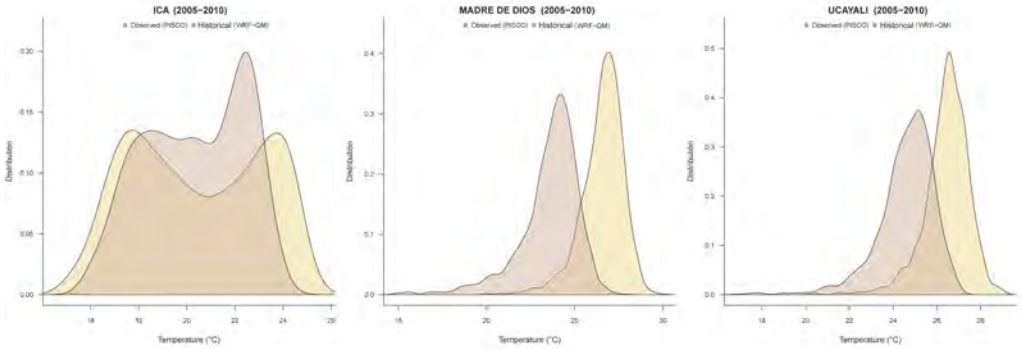

Figure A.2: Comparison of the distribution of the simulated (historical) and observed temperature values for the period 2005 to 2010. The distribution of the observed temperatures is highlighted in yellow while the historical values are indicated with brown color.

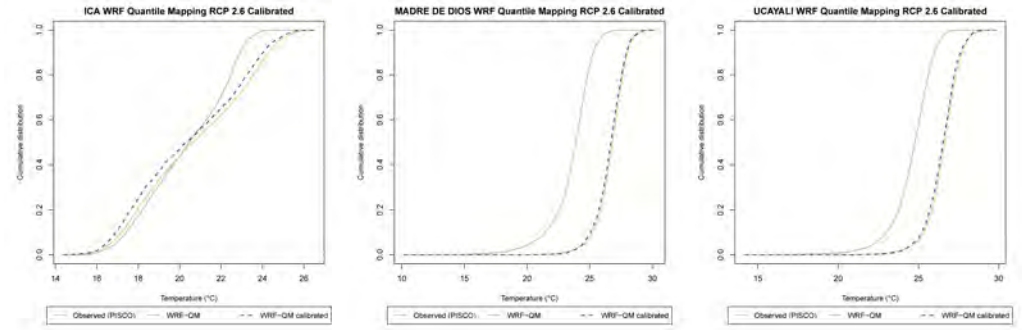

Figure A.3: Cumulative distribution of the simulated (RCP 2.6), observed and calibrated temperature values. The cumulative distribution of the calibrated series is represented by a dotted line.

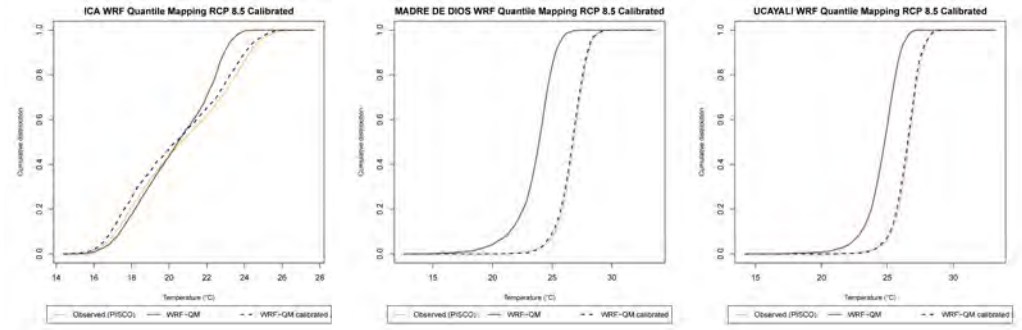

Figure A.4: Cumulative distribution of the simulated (RCP 8.5), observed and calibrated temperature values. The cumulative distribution of the calibrated series is represented by a dotted line.

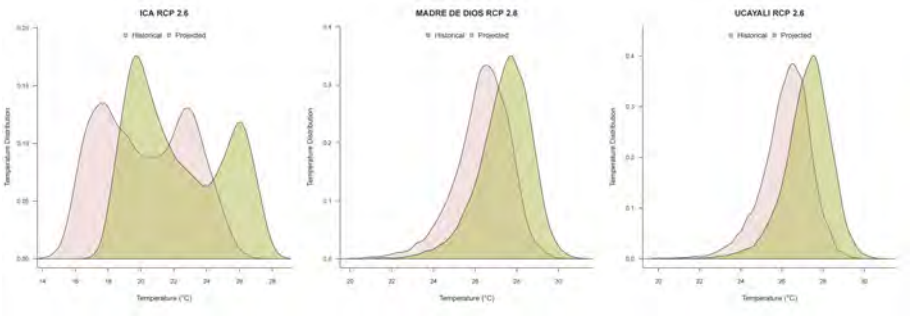

Figure A.5: Comparison of the distribution of the historical temperature series (1981-2010) with the projected temperature series simulated under RCP 2.6 (1971-2099). Both series are calibrated. The distribution of the historical temperature is highlighted in light pink. Additionally, the projected temperature values are indicated in green colour.

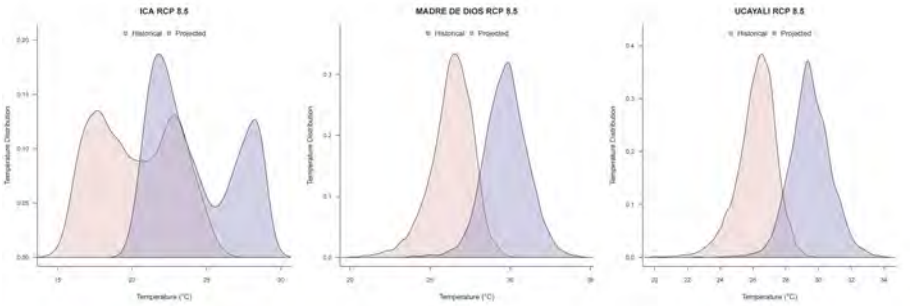

Figure A.6: Comparison of the distribution of the historical temperature series (1981-2010) with the projected temperature series simulated under RCP 8.5 (1971-2099). Both series are calibrated. The distribution of the historical temperature is highlighted in pink. Additionally, the projected temperature values are indicated in purple.

Table A.1: Estimated number of deaths (AN) used to calculate the attributable mortality fraction (AF) for the period 2071 to 2099. The estimation of AN was done for the historical (1981-2010) and for the future period (2071-2099) under two scenarios. The estimated number of deaths was calculated for the cold and heat component, as well as the total.

Projected Attributable Number (n)						
	Historical			**Future**		
	Total			**Total**		
	Ica	Madre de Dios	Ucayali	Ica	Madre de Dios	Ucayali
WRF-QM-2.6	1329 [730 : 1957]	139 [-170 : 427]	283 [-417 : 934]	1521 [876 : 2120]	157 [-37 : 332]	321 [-119 : 688]
WRF-QM-8.5				2539 [1495 : 3415]	1127 [226 : 1763]	2441 [339 : 3893]
	Cold			**Cold**		
	Ica	Madre de Dios	Ucayali	Ica	Madre de Dios	Ucayali
WRF-QM-2.6	1290 [692 : 1922]	127 [-186 : 417]	260 [-438 : 912]	790 [337 : 1252]	67 [-119 : 239]	135 [-259 : 496]
WRF-QM-8.5				457 [158 : 748]	6 [-13 : 24]	10 [-20 : 37]
	Heat			**Heat**		
	Ica	Madre de Dios	Ucayali	Ica	Madre de Dios	Ucayali
WRF-QM-2.6	39 [17 : 63]	12 [-1 : 25]	23 [-2 : 48]	730 [396 : 1048]	89 [8 : 166]	186 [11 : 359]
WRF-QM-8.5				2082 [1227 : 2833]	1121 [219 : 1743]	2432 [342 : 3871]

Acknowledgements

This master's thesis is an achievement that would not have been possible without the guidance, support and friendship of many remarkable people.

First of all, I want to express my gratitude to Professor Dr. Ana María Vicedo-Cabrera, who introduced me to the fascinating field of Environmental Epidemiology and Public Health Science. Thank you for the guidance, time and support through this journey. Specially, thank you for the knowledge you always shared and the ideas that you provided me to improve this project.

Many thanks to Dr. Coral Salvador and Dr. Evan de Schrijver, who always shared their time and knowledge. Thank you Coral for always offering not just your time but also for your friendship. Thank you Evan for taking the time of answering questions, explaining complex concepts and for always spreading positivity at the office.

I would also like to express my gratitude to the co-supervisor of this work, Dr. Santos J. González Rojí. Thank you for taking the time to review this project, share your work and provide valuable comments.

Additionally, I want to thank Prof. Christoph Raible for taking the time to chair my thesis defence and, to Dr. Peter Stucki for the support and advice that was given during my studies.

Moreover, to my non-official advisor, Adrian Huerta, who always shared his ideas to improve this master's thesis. Thank you for providing the insights of the PISCOt v1.2 dataset and the time to share the beautiful culture of Peru.

Special thanks to the Health Ministry of Peru for their cooperation in providing the recorded mortality datasets for this project.

Furthermore, I acknowledge the partial funding for my studies granted by the Na-

tional Council of Sciences, and Technology (CONACYT) of Mexico.

Lastly, my wholehearted gratitude and appreciation to:

- Classmates from the Climate Sciences program, for the time, friendship and support during all the time we shared. Specially to Paul Alva, Leonardo Quirino, Andrea Angelidou, Sina Aregger, Henrique Traeger, Nicolás Duque, Edgar Dolores, Gabriela Espejo and Laurel Faher.
- Climate Change and Health research group, Sidharth Sivaraj, Adrienne Wehrli, Sujung Lee, Lilian Goepp, Carol Bouverat and Nadine Lötscher, for always sharing knowledge, stories and for the support in preparation for my thesis defence.
- Sereina Richner, Susana Zarzoza and Sandra Garcia, for the friendship and constant encouragement.
- My parents, Marina Olvera and Tiburcio Hidalgo, for always believing in me and and providing a lifetime of unwavering support in everything I pursue.

Centzompa, Tlasohkamati in yóllotl.

UNIVERSITÄT
BERN

OESCHGER CENTRE
CLIMATE CHANGE RESEARCH

Declaration of consent

on the basis of Article 30 of the RSL Phil.-nat. 18

Name/First Name:	Katia Karen Hidalgo Olvera
Registration Number:	21-116-074
Study program:	Master in Climate Sciences
	Bachelor ☐ Master ☑ Dissertation ☐
Title of the thesis:	Temperature-mortality projections under climate change scenarios in Peru
Supervisor:	Prof. Dr. Ana María Vicedo-Cabrera
Co-supervisor:	Dr. Santos José González Rojí

I declare herewith that this thesis is my own work and that I have not used any sources other than those stated. I have indicated the adoption of quotations as well as thoughts taken from other authors as such in the thesis. I am aware that the Senate pursuant to Article 36 paragraph 1 litera r of the University Act of 5 September, 1996 is authorized to revoke the title awarded on the basis of this thesis.

For the purposes of evaluation and verification of compliance with the declaration of originality and the regulations governing plagiarism, I hereby grant the University of Bern the right to process my personal data and to perform the acts of use this requires, in particular, to reproduce the written thesis and to store it permanently in a database, and to use said database, or to make said database available, to enable comparison with future theses submitted by others.

Place/Date

Zurich, 11. 9. 2024: